A spectroscopic investigation of polyacetylenic molecules in the molluskan biogenic matrix

by

Werner Barnard

Submitted in partial fulfillment of the requirements for the degree

Magister Scientiae

In the Faculty of Natural and Agricultural Sciences, University of Pretoria

August 2005

Acknowledgements

I would like to thank the following people who have supported and assisted me during the completion of this degree:

- My supervisor, Prof. Danita De Waal, without your support and belief in this project it would have never seen daylight.
- My parents for helping where they possibly could, even if it meant collecting much needed samples at 04:00 in the morning.
- Prof. Jan Boeyens for constructive input and support during this project.
- The National Research Foundation (NRF) for financial assistance.
- The Molecular Spectroscopy Research group for all their constructive discussions and helpful hints.
- Daniela Bezuidenhout, because without your company and social support during late nights and early mornings, research would be less than enjoyable.
- My dearest friends Riaan du Plessis, who tried to understand what I was saying, but never really did, and Denise Dale who understood what I said in her own special way, but always worried more about the goings on of foreign stellar systems, my utmost of gratitude for both your support in all facets of this project and my life.

"And in like manner we see the race of shells painting
the lap of earth, where with gentle waves the sea beats
on the thirsty sand of the winding shore.
And so I must insist these things must be:
The atoms are by nature made, not all alike,
not turned out by factory's mass production.
Differ then they must."

Lucretius, II, 374 – 380

Abstract:

A spectroscopic investigation of polyacetylenic molecules in the molluskan biogenic matrix

by

Werner Barnard

Supervisor: Prof. D. de Waal
Submitted in partial fulfillment of the requirements for the degree Magister Scientiae
Department of Chemistry, University of Pretoria, Pretoria

Molluscan shells show great diversity in colour, which is due to many different classes of chemical compounds. The identification of the pigments found in the molluscan shells of a diverse group of marine species was done *in situ* using Resonance Raman spectroscopy, and found to be unsubstituted polyacetylenes.

Two South African species (*D. serra* and *J. janthina*) were chosen for extraction of the pigment-containing organic component, and it was found that the vibrational bands in the Raman spectra of the extracted component shifted relative to that obtained in the molluscan matrix, indicating structural changes in the pigmentary molecules upon extraction.

Published correlations were used to evaluate the possible length of the conjugated chain, and a new correlation was established using previous reported data. The conjugated chain length predicted from the new correlation of the studied pigmentary molecules ranges between ten and twelve double bonds.

Samevatting:

A spectroscopic investigation of polyacetylenic molecules in the molluskan biogenic matrix

deur

Werner Barnard

Promotor: Prof. D. de Waal

Voorgelê ter vervulling van 'n deel van die vereistes vir die graad Magister Scientiae

Departement Chemie, Universiteit van Pretoria, Pretoria

Weekdier skulpe toon 'n groot verskeidenheid in kleur as gevolg van verskillende chemiese verbindings. Die identifikasie van die pigmente wat in 'n verskeidenheid weekdierspesies se skulpe gevind word, is *in situ* gedoen deur middel van Resonans Raman spektroskopie. Die pigmente is geïdentifiseer as ongesubstitueerde poliasetileen molekules.

Twee Suid-Afrikaanse spesies (*D. serra* en *J. janthina*) is gekies om pigmenthoudende organiese deel te ekstraeer. Die vibrasie bande in die Raman spektra van die geëkstraeerde deel het geskuif relatief tot die vibrasie band posisies verkry in die skulp matriks, wat aanduidend is van strukturele veranderinge in die pigment molekules as gevolg van die ekstraksie.

Gepubliseerde verwantskappe was gebruik om die moontlike lengte van die gekonjugeerde ketting te bepaal, en 'n nuwe verwantskap is verkry deur gebruik te maak van voorheen gepubliseerde data. Die lengte van konjugasie wat voorspel is deur die nuwe verwantskap vir die pigment molekules wat bestudeer is, is tussen tien en twaalf dubbelbindings.

TABLE OF CONTENTS

List of Figures

List of Tables

List of Related Achievements

Poster Presentations

1. "$CaCO_3$ – An Inorganic Key To Better Raman Spectra Of Organic Compounds In The Future?" W. Barnard and D. De Waal, *SACI 2003 Inorganic Conference*, Pretoria, South Africa, 8 – 11 June 2003, awarded 2nd place.

Oral Presentations

1. "Raman Investigation of Molluscan Carotenoid Pigments" *SASS Young Spectroscopists Symposium*, Rand Afrikaans University, 12 August 2003, awarded 1st place.

2. "Raman Investigation of Molluscan Carotenoid Pigments" *SACI/RSC Young Chemist Symposium*, University of the Witwatersrand, 24 October 2003, awarded 2nd place.

3. "Raman Ondersoek van Skulpdier Karotenoïed Pigmente" *SAAWK Studente Simposium*, University of the Free State, 31 October 2003, awarded Bronze D.M. Kisch Merit Medal.

4. "Polyacetylenic Molecules in the Molluscan Shell Matrix" *SACI 2004, The 37th National Convention of the South Arican Chemical Institute*, Pretoria, South Africa, 4 – 9 July 2004.

Chapter 1

Introduction

1.1 Molluscan Pigments

Nature has never disappointed in the use of pigmentary molecules for colour in the fauna and flora kingdoms. For centuries mankind has harvested and used these colouring agents to adorn themselves or beautify their clothing. One of the most prized of these colouring agents was Tyrian purple (6,6'-dibromoindigo), and was obtained from molluscs belonging to either the genus Muricidae or Thaisidae[1].

The pigmentary molecules responsible for the colouration of specifically the molluscan shell was particularly difficult to determine relative to that of the soft parts of a mollusc – the reason being the difficulty in extraction of the pigment. Some early methods[2] report the use of 6*N* HCl solutions at 70ºC, compared to a simple ether or acetone extraction for the soft tissue parts. Granted, some chemical compounds, might be stable under these conditions, but many may not be. 'Softer' methods entailed the digestion of the mainly $CaCO_3$ molluscan shell by means of Na_2EDTA, or 5% HCl in acetone. These methods, first used on corals[3], were later employed, and proved successful in the extraction of the pigment from the molluscan shell[4,5,6].

Different types of pigmentary molecules in different parts of the molluscan body have been identified using various techniques such as UV-Visible spectroscopy[7], column chromatography[8,9] and HPLC[10]. The most important of these pigments include the carotenoids, indole pigments (indigoids and melanins), tetrapyrroles (porphyrins and bilichromes) and hemocyanins. Of these, carotenoids offer the strongest link to terrestrial life as they are found in

many plants and land animals, not part of the phylum Mollusca, as colouring agents. The majority of pigments so far identified in molluscan shells seems to be of carotenoid nature[4,5,6].

Carotenoids can be described as relatively short linear polyene chains with substituents. The common chemical denominator for all classical carotenoids is the tetramethyl substituted polyene backbone shown in Figure 1-1. The structures of some of the more common carotenoids are shown in Figure 1-2.

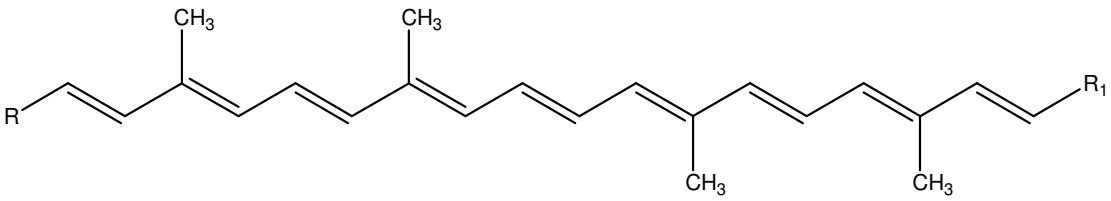

Figure 1-1: The classical carotenoid polyene backbone showing the positions of the four methyl groups.

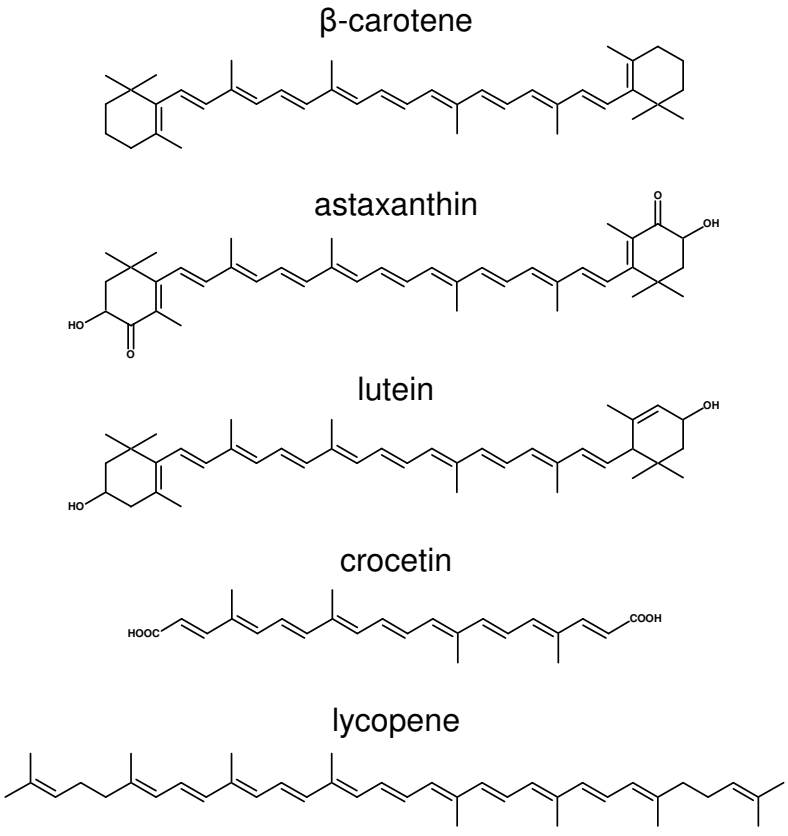

Figure 1-2: Structures of some common carotenoids showing different terminal group functionalities.

Carotenoids are of great industrial importance in the food industry for both their nutritional and aesthetical value. Two industries that use it as an important additive in feedstock is the poultry and salmon fishing industry, for both the aforementioned reasons, and have therefore done extensive research to find a more economically viable source of the required carotenoids[11,12,13].

1.2 The Molluscan Shell

The molluscan shell is an excellent example of what is known as a biogenic matrix that consists of both an organic and inorganic component. The organic component is largely made up of the conchoilin-proteins that hold the inorganic part of the matrix together[14]. Also part of the organic component is the all-important pigment of the shell. It is usually only found deposited on the surface of the shell, be it internally or externally.

The major component of the molluscan shell is the inorganic part that is largely made up of $CaCO_3$, but Mg^{2+}, Sr^{2+} can also be found in significant quantities[15]. Other minor trace elements such as iron and magnesium have also been reported to be present[14,15]. $CaCO_3$ itself can be found in three different phases, which are calcite, aragonite and vaterite[16]. The two dominant phases seem to be calcite and aragonite, and can either occur separately or in combination with one another in the molluscan shell[14,15]. The carbonate phase of the shell seems to be dependent on many factors[14], but the most important seems to be the conchoilin composition to initialise the biomineralisation process[17].

1.3 The use of Raman Spectroscopy

Raman spectroscopy has been developed as a powerful, non-destructive tool for the *in situ* observation or identification of chemical compounds. Raman spectroscopy also becomes the preferred method of investigation when it comes to very complex, inhomogeneous samples as it can be utilised as a

micro probing technique. The sample is simply placed under the microscope and the laser focused on the desired area for which a spectrum needs to be obtained. Very little sample preparation is usually required for Raman spectroscopy, and it has therefore become the desired technique when working with valuable or microscopic samples that need to be investigated *in situ* or *in vivo*.

A good example of this is the study or verification of archaeological samples and historical artworks[18]. Raman spectroscopy has also found wide application in the biological field for *in situ* or *in vivo* studies and diagnostic purposes[19,20]. Carotenoids have favourably lent themselves as the ideal molecule for such studies, as they show a dramatic Resonance Raman (RR) effect with blue to green laser wavelengths. This enables scientists to detect carotenoids at very low concentrations in complex biological mixtures if the incident laser wavelength is selected correctly. One such successful example is the use of this technique for the probing of carotenoids *in vivo* in living human subjects for the early detection of certain skin and retinal problems[21,22,23].

Carotenoids also have the favourable property that they do not show an appreciable fluorescence with blue to green laser wavelengths, thus reducing the necessity of spectral corrections. Furthermore, many low intensity vibrational bands can be enhanced, making it easier to be distinguished. The major reason for the lack of fluorescence for carotenoids is the preferred pathways of relaxation that exists after excitation by the incident wavelength[23]. From Figure 1-3 it can be seen that after optical excitation from the 1^1A_g ground state to the 1^1B_u excited state, three pathways of relaxation exist for the molecule: The first being the Raman effect itself, and the other two pathways is either the fluorescent relaxation, or the nonradiative relaxation to another excited state, the 2^1A_g state, found below the 1^1B_u state. Once relaxation has occurred using the latter pathway, an electronic transition from the 2^1A_g state to the 1^1A_g ground state is parity forbidden[23]. Unfortunately,

many of the biological matrices in which the carotenoids are found, fluoresce which can become a problem.

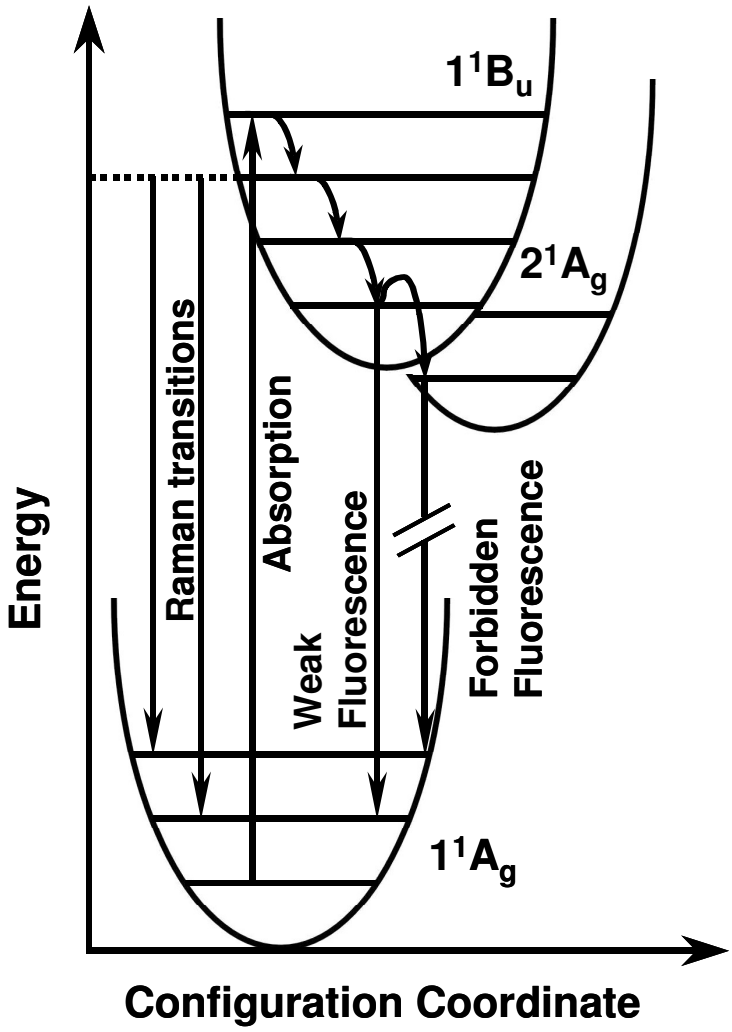

Figure 1-3: Diagram[23] showing the different pathways of relaxation to the ground state that occurs in most carotenoids after excitation to an excited state.

As $CaCO_3$ is the major component of the molluscan shell, the problem of matrix fluorescence is eliminated in the Raman spectrum of the molluscan shell pigment. The positions of the Raman bands of $CaCO_3$ do not interfere with those of the carotenoid, and no Resonance Raman effect is observed for it in the blue to green wavelength region. The strong symmetrical stretching mode of the CO_3^{2-} ion acts as a good internal reference in the obtained spectra. The stability of the pigment in the matrix is also favourable, allowing for acceptable spectra to be obtained without any visible degradation[24].

Taking into account all these aspects, Raman spectroscopy seems to be the most favourable technique with which to investigate the pigments of molluscan shells *in situ*.

1.4 References

1. C.J. Cooksey, *Molecules*, 2001, **6**, 736 – 769.
2. D.L. Fox, *Pigmentation of Molluscs* in *Physiology of Mollusca Volume II*, K.M. Wilbur, C.M. Yonge (Eds), 1st Edition, Academic Press, New York, 1966, Chapter 8 and references incl.
3. H. Ronneberg, D.L. Fox, S. Liaaen-Jensen, *Comp. Biochem Physiol.*, 1978, **64B**, 407 – 408.
4. J.C. Merlin, M.L. Delé-Dubois, *Bull. Soc. Zool. France*, 1983, **108**, 289 – 301.
5. J.C. Merlin, M.L. Delé-Dubois, *Comp. Biochem. Physiol.*, 1986, **84B**, 97 – 103.
6. J.C. Merlin, *Pure & Appl. Chem.*, 1985, **57**, 785 – 792.
7. A. Vershinin, *Comp. Biochem. Physiol.*, 1996, **113B**, 63 – 71.
8. H. Ronneberg, G. Borch, D.L. Fox, S. Liaaen-Jensen, *Comp. Biochem Physiol.*, 1978, **62B**, 309 – 312.
9. H. Berger, H. Ronneberg, G. Borch, *Comp. Biochem. Physiol.*, 1982, **71B**, 253 – 258.
10. M. Cusack, G. Curry, H. Clegg, G. Abbott, *Comp. Biochem. Physiol.*, 1992, **102B**, 93 – 95.
11. J.A. Del Campo, J. Moreno, H. Rodríguez, M.A. Vargas, J. Rivas, M.G. Guerrero, *J. Biotech.*, 2000, **76**, 51 – 59.
12. J. Hudon, *Biotech. Adv.*, 1994, **12**, 49 – 69.
13. J.P. Wold, B.J. Marquardt, B.K. Dable, D.R. Robb, B. Hatlen, *Appl. Spectroscopy*, 2004, **58**, 395 – 403.
14. K.M. Wilbur, *Shell Formation and Regeneration* in *Physiology of Mollusca Volume I*, K.M. Wilbur, C.M. Yonge (Eds), 1st Edition, Academic Press, New York, 1964, Chapter 8.

15. G.P. Hawkes, R.W. Day, M.W. Wallace, K.W. Nugent, A.A. Bettiol, D.N. Jamieson, M.C. Williams, *Journal of Shellfish Research*, 1996, **15**, 659 – 666.
16. C.G. Kontoyannis, N.V. Vagenas, *The Analyst*, 2000, **125**, 251 – 255.
17. C.E. Bowen, H. Tang, *Comp. Biochem. Physiol.*, 1996, **115A**, 269 – 275.
18. R.J.H. Clark, *Vibrational Spectroscopy of Colours, Dyes and Pigments* in *Handbook of Vibrational Spetroscopy Volume 4*, J.M. Chalmers, P.R. Griffiths (Eds), John Wiley & Sons, Chichester, 2002.
19. T.G. Spiro (Ed.), *Biological Applications Of Raman Spectroscopy Volume 1*, John Wiley & Sons, New York, 1987.
20. T.G. Spiro (Ed.), *Biological Applications Of Raman Spectroscopy Volume 2*, John Wiley & Sons, New York, 1987.
21. I.V. Ermakov, R.W. McClane, W. Gellermann, *Optics Letters*, 2001, **26**, 202 – 204.
22. I.V. Ermakov, M.R. Ermakova, R.W. McClane, W. Gellermann, *Optics Letters*, 2001, **26**, 1179 – 1181.
23. W. Gellermann, I.V. Ermakov, M.R. Ermakova, R.W. McClane, *J. Opt. Soc. Am.*, 2002, **19**, 1172 – 1186.
24. R. Withnall, B.Z. Chowdry, J. Silver, H.G.M. Edwards, L.F.C. de Oliveira, *Spectrochimica Acta*, 2003, **59A**, 2207 – 2212.

Chapter 2

Theoretical Aspects

2.1 The Theory of Vibrational Spectroscopy[1]

The energy of any polyatomic system can be separated in four main quantised components. These are the energies associated with the translational motion, the electrons, the vibrations and the rotations of the polyatomic unit:

$$E_T = E_{trans} + E_{e^-} + E_{vib} + E_{rot} \tag{2.1}$$

Of these, only E_{e^-}, E_{vib} and E_{rot} are usually of interest to the molecular spectroscopist. The relationship between these three energies for a diatomic unit is illustrated in Figure 2-1. Here only the vibrational energy will be discussed. The two complementary techniques that are most often employed in obtaining vibrational information are Infrared and Raman spectroscopy, but the origins of these two underlying phenomena are very different.

2.1.1 Infrared (IR) Spectroscopy

The electric dipole moment μ of a chemical bond can be described as

$$\mu = qd \tag{2.2}$$

where q is the charge product at one pole and d the distance between the poles. As a molecular bond vibrates, the rate of change in the dipole moment is the same as the frequency of the bond vibration. For a polyatomic molecule

having a permanent dipole, $\mu \neq 0$ at any given moment during the vibration. Because quantum mechanics show that molecular vibrational energy levels are quantised, the dipole moment will only couple with the electric field of the infrared radiation that matches the correct frequency of vibration of the molecule, allowing for an absorption and emission of infrared photons between two vibrational energy levels in the molecule's electronic ground state. Infrared spectroscopy is therefore a measurement of the frequency during the change of the permanent dipole moment as the molecule vibrates.

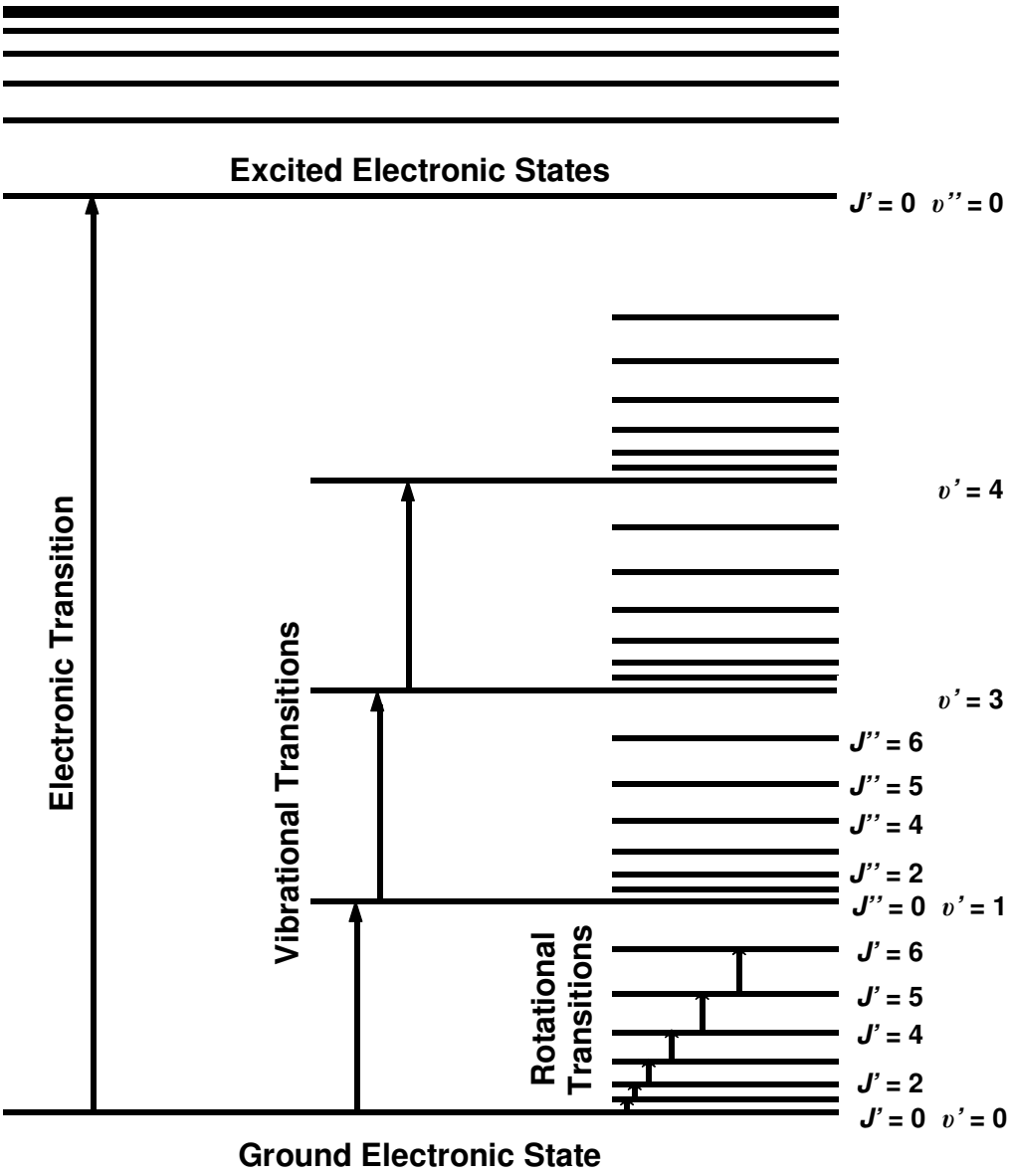

Figure 2-1: Schematic showing the relationship of the electronic, vibrational and rotational energy levels for a diatomic unit[1]. Not drawn to scale.

2.1.2 Raman Spectroscopy

In Raman spectroscopy, we observe electromagnetic radiation, usually visible light, scattered by molecules when it is irradiated with a monochromatic light source. The source of the monochromatic radiation is usually a laser set to a specific frequency. When the light is scattered by the molecule, two possible scattering processes can occur: elastic and inelastic scattering of the light. The elastic scattering process is when the frequency of the light scattered by the molecule is equal to the frequency ν of the incident light, and is called Rayleigh scattering. This is by far the major effect observed. When light is scattered inelastically by a molecule, the frequency of the light scattered by the molecule changes to a frequency ν_i. If $\nu_i < \nu$ the scattered radiation is called Stokes radiation, and if $\nu_i > \nu$ it is called anti-Stokes radiation. The difference $\nu_0 = |\nu - \nu_i|$, corresponds to frequencies or energies in the infrared region. In both the inelastic and elastic scattering process the molecule is excited to a virtual state. These virtual states can be seen as being a sum over all excited states, when we look at Raman as a two photon process. This entails the virtual absorption of the first photon to numerous excited vibrational states, whereafter the second photon is virtually emitted to return to the ground state[2,3]. These virtual states do not correspond to true vibrational or electronic levels, as molecules have a continuum of virtual states dependent only on the frequency of the exciting laser.

Molecules that are centrosymmetric or those with high symmetry such that the vector sum of the individual bond dipoles gives $\mu = 0$, will have no permanent dipole, even though each bond might have a nonzero dipole moment associated with it. When a molecule is placed in an electric field E a dipole moment μ_i is induced, with

$$\mu_i = \alpha E \tag{2.3}$$

where the proportionality constant α is called the polarizability. The electric field E has an associated fluctuation frequency v, and therefore it can be expressed as

$$E = E_0 \cos 2\pi v t \tag{2.4}$$

with amplitude E_0 over time t. The induced dipole in the electric field can now be expressed as

$$\mu_i = \alpha E_0 \cos 2\pi v t \,. \tag{2.5}$$

The displacement x of the atoms from the equilibrium position, vibrating at a frequency v_0 can be expressed as

$$x = x_0 \cos 2\pi v_0 t \,, \tag{2.6}$$

and because polarizability is a molecular property, it is also dependent on the displacement from the equilibrium position and will vary according to the vibrational frequency of the molecule giving:

$$\begin{aligned} \alpha &= \alpha_0 + \left(\frac{\partial \alpha}{\partial x}\right)_0 x \\ &= \alpha_0 + \left(\frac{\partial \alpha}{\partial x}\right)_0 x_0 \cos 2\pi v_0 t \end{aligned} \tag{2.7}$$

where α_0 is the polarizability at equilibrium, and $(\partial\alpha/\partial x)_0$ is the rate of change of α during the change of x at the equilibrium position. Substituting Eq. 2.7 into Eq. 2.5 yields

$$\mu_i = \left[\alpha_0 + \left(\frac{\partial \alpha}{\partial x}\right)_0 x_0 \cos 2\pi v_0 t\right]\left[E_0 \cos 2\pi v t\right]. \tag{2.8}$$

Use of the identity cosAcosB = (1/2)[cos(A+B) + cos(A-B)], after the rearrangement of Eq. 2.8, finally gives

$$\mu_i = \alpha_0 E_0 \cos 2\pi\nu t + \frac{1}{2}\left(\frac{\partial\alpha}{\partial x}\right)_0 x_0 E_0 \{\cos[2\pi(\nu+\nu_0)t] + \cos[2\pi(\nu-\nu_0)t]\}. \quad (2.9)$$

The first term in Eq. 2.9 refers to the elastic Rayleigh (ν) scattering while the last term refers to the two inelastic processes of anti-Stokes ($\nu + \nu_0$) and Stokes ($\nu - \nu_0$) scattering. In Figure 2-2 the relationships between the different vibrational processes are clearly indicated. Because Raman spectroscopy measures a difference between the incident and scattered light, the positions of the vibrational bands are not dependent on the wavelength of laser excitation.

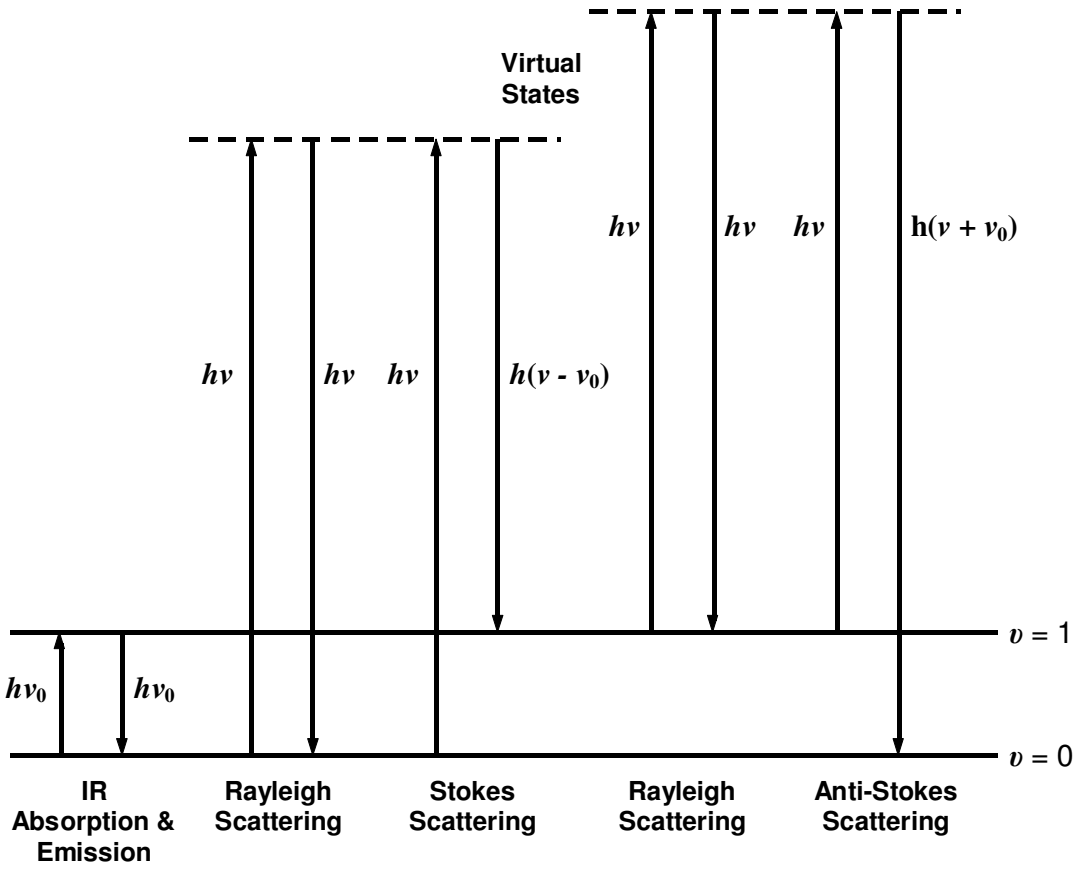

Figure 2-2: Schematic showing the relationships between the different vibrational processes.

The Stokes scattering intensities are more intense than those of the anti-Stokes scattering. The explanation for this can be found in the populations of the different vibrational energy levels. From the Maxwell-Boltzmann distribution law, the relative populations of two energy levels in a harmonic oscillator with associated energies ε_A and ε_B ($\varepsilon_A < \varepsilon_B$), having degeneracies g_A and g_B is

$$\frac{n_B}{n_A} = \frac{g_B}{g_A} e^{-\Delta\varepsilon / kT} \tag{2.10}$$

where n_A and n_B are the molecule populations in each state, k is Boltzmann's constant and T is the temperature in Kelvin. Because vibrational levels are nondegenerate $g_A = g_B = 1$, and between any two consecutive vibrational levels $\Delta\varepsilon = h\nu_0$, giving

$$\frac{n_{\upsilon+1}}{n_\upsilon} = e^{-h\nu_0 / kT}. \tag{2.11}$$

Stokes scattering originates from the $\upsilon = 0$ vibrational level whereas anti-Stokes scattering originates from the $\upsilon = 1$ vibrational level. Evaluation of real experimental data with Eq. 2.11 will show that the vibrational levels are rarely populated above the $\upsilon = 0$ level at room temperature, thus explaining the difference in intensities observed. Spectroscopists therefore usually obtain the Stokes spectrum.

2.1.2.1 Overtone and Combination Bands

The quantum mechanical treatment of the harmonic oscillator has lead to the conclusion that vibrational energy levels are quantised and that the selection rule allows for transitions of only the kind $\Delta\upsilon = \pm 1$. The transition from $\upsilon = 0$ to $\upsilon = 1$ is called the fundamental transition. Overtones are defined as vibrational bands that are integer multiples of the fundamental transition, and combination bands are either the difference or sum of two fundamental bands.

Both are forbidden by the selection rule, but because of the anharmonicity of true molecules that deviate from the harmonic oscillator model, they are sometimes observed. For a harmonic oscillator the potential curve is given by

$$V = \tfrac{1}{2} kx^2 \tag{2.12}$$

where k is the force constant. For systems that deviate from the harmonic model, a better approximation can be made using

$$V = \tfrac{1}{2} kx^2 - gx^3 \qquad (k >> g) \tag{2.13}$$

with corresponding eigenvalues

$$E_\upsilon = hc\omega_e(\upsilon + \tfrac{1}{2}) - hcx_e\omega_e(\upsilon + \tfrac{1}{2})^2 + \ldots \tag{2.14}$$

We can approximate the anharmonicity corrected wavenumber ω_e and the anharmonicity magnitude $\omega_e x_e$ by rearranging Eq. 2.14 to give

$$(E_\upsilon - E_0)/hc = \upsilon\omega_e - x_e\omega_e(\upsilon^2 + \upsilon) + \ldots \tag{2.15}$$

with

Fundamental : $\nu_1 = \omega_e - 2x_e\omega_e$

1st overtone : $\nu_2 = 2\omega_e - 6x_e\omega_e$

2nd overtone : $\nu_3 = 3\omega_e - 12x_e\omega_e$

Knowing ω_e we can more accurately approximate the force constant k using

$$k = 4\pi^2 c^2 \omega_e^{\,2} \mu \tag{2.16}$$

where c is the speed of light, and μ is the reduced mass of the two atoms involved in the bond.

2.1.2.2 Resonance Raman (RR) Spectroscopy

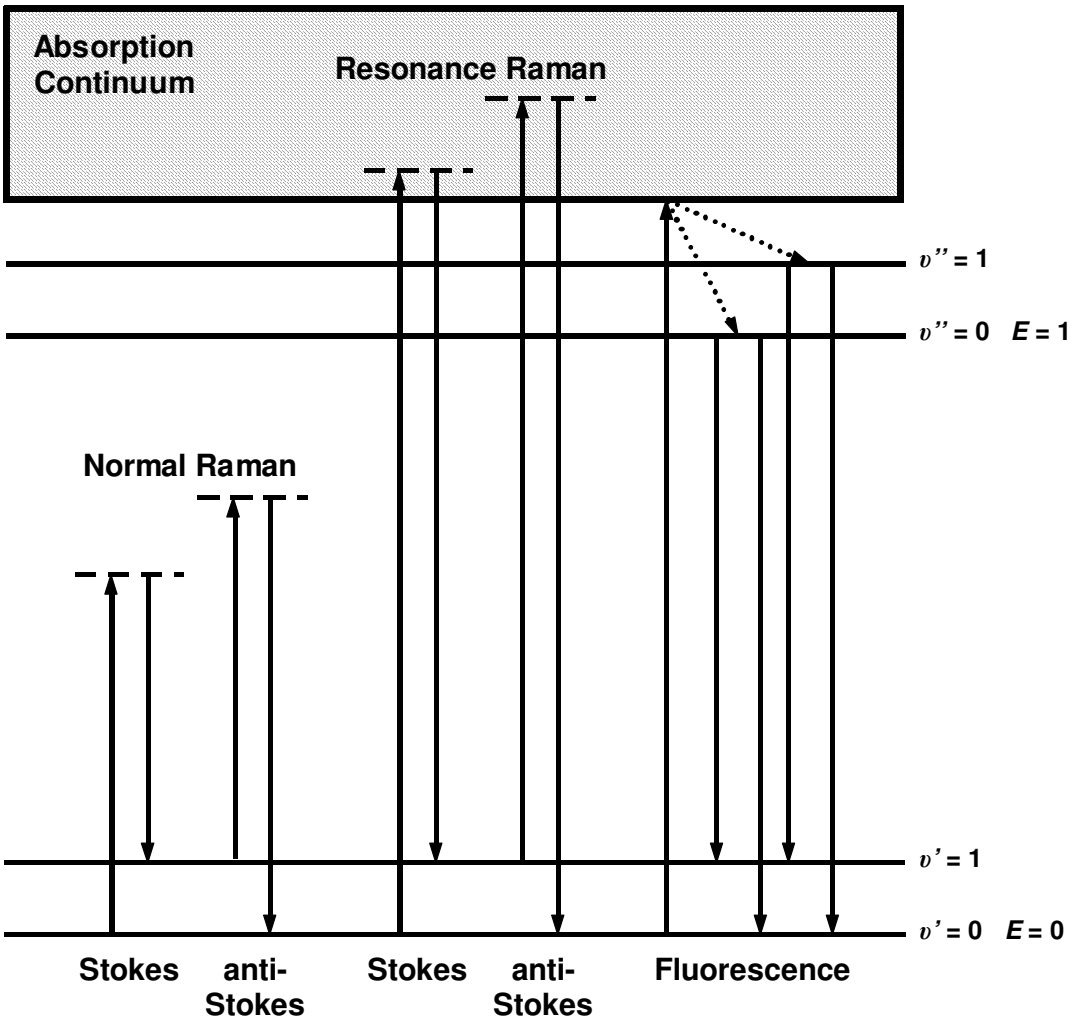

Figure 2-3: The processes of Normal and Resonance Raman as well as fluorescence which can occur during irradiation by laser light.

When the energy of the laser wavelength used for excitation, is such that it is coincides with the energy of an electronic transition of the molecule, the RR effect can occur. In other words, the virtual state energies of the Raman effect approaches that of the electronic excited states. When this occurs, the polarizability of the electron cloud of the molecule increases, creating a higher probability for the Raman transition to occur[4]. Returning to the sum-over-states approximation, the resonant electronic state terms are seen to dominate the sum-over-states expression for the virtual states, making the

nonresonant terms negligible[2]. This results in an increase of the intensity of certain Raman bands by as much as 10^6 times[2,3]. At the same time the less desired effect of fluorescence can also occur. Figure 2-3 illustrates the difference between normal and resonance Raman scattering, and fluorescence. If combination and overtone bands that originate from the resonance enhanced fundamentals are observed, their intensities are also enhanced by the resonance effect.

2.2 The Effective Conjugation Coordinate (ECC) Theory for Polyenes[5]

The use of ECC theory has become the preferred method of modeling polyconjugated systems, as it has been successfully applied to chemically different conjugated systems such as polyacetylene[5,6,7], dithienothiophene derivatives[8], polyaromatic polymers[5,9] and conjugated polymers consisting of heteroatomic units[5,9]. Polyacetylene has been the most studied of these systems, and the different chemical variations of the finite and infinite polyconjugated chain for both the doped and undoped forms correlate well with the theory[5,6,7]. For polyacetylene, the simplest system is neutral, undoped all-*trans* polyacetylene.

ECC theory is a generalized reformulation of Amplitude Mode (AM) Theory[9]. Originally AM Theory gave a good simplified model of polyacetylene, but could not be applied to doped polyacetylene systems[9]. ECC theory defines coordinates that describe the electron-phonon coupling that occurs between the conjugated π-electrons and the molecular geometry[7,10]. We can define the symmetry coordinates for polyacetylene using the internal coordinates as defined in Fig 2-4 relative to the point group C_{2h} [5].

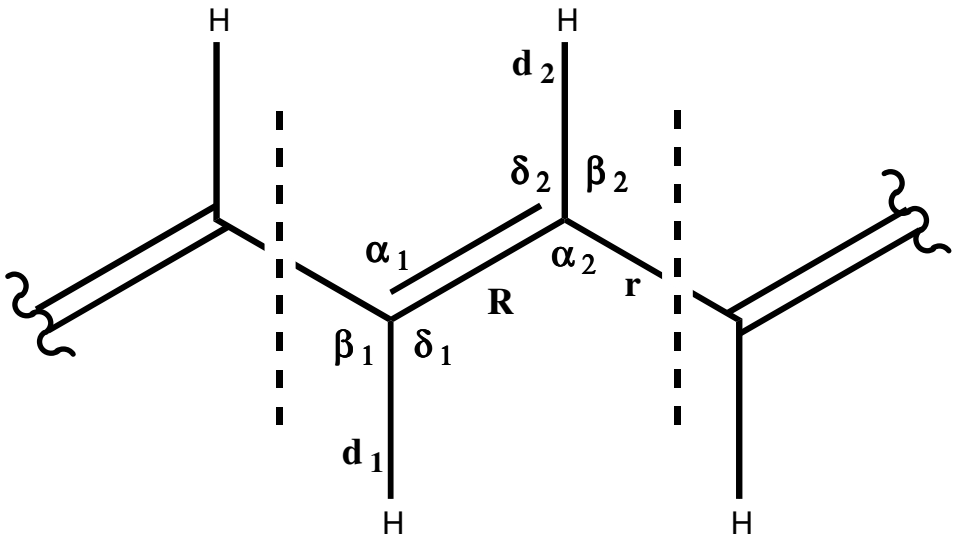

Figure 2-4: The internal coordinates as defined for the repeating unit of polyacetylene in the C_{2h} all-*trans* configuration[5].

For the a_g mode the most used coordinate is the 'effective conjugation coordinate' $Я$. For a finite chain with N C=C bonds and M C-C bonds it is defined as:

$$Я = \left(N_{C=C} + M_{C-C}\right)^{-1}\left(\sum_{n=1}^{N_{C=C}} R^{(n)}{}_{C=C} - \sum_{n=1}^{M_{C-C}} r^{(n)}{}_{C-C}\right) \qquad (2.17)$$

Where $R^{(n)}{}_{C=C}$ and $R^{(n)}{}_{C\text{-}C}$ are the lengths of the nth carbon double and single bonds respectively. Extending to the infinite chain $Я$ becomes

$$Я = {}^{1}\!/_{\sqrt{2}}\left(R_{C=C} - r_{C-C}\right). \qquad (2.16)$$

A full description for the symmetry coordinates of the four a_g modes of *trans*-polyacetylene can be obtained upon defining the following three coordinates together with $Я$[5]:

$$R^{+} = {}^{1}\!/_{\sqrt{2}}\left(R_{C=C} + r_{C-C}\right) \qquad (2.17)$$

$$d^{+} = {}^{1}\!/_{\sqrt{2}}\left(d_1 + d_2\right) \qquad (2.18)$$

$$W^{+} = \tfrac{1}{2\sqrt{2}}\left(\beta_1 + \beta_2 - \delta_1 - \delta_2\right) \tag{2.19}$$

d, β and δ are defined in Fig 2-4. Both $Я$ and R^{+} contribute to the C=C, C-C and HC=CH vibrational modes in different degrees[5], but modes that are dominant in the Raman spectrum are those skeletal modes that have the largest electron-phonon coupling[11], and in the case of polyacetylene these are the C=C and C-C stretching modes[5,11]. If any change were to occur in the frequencies of these normal modes involved in the carbon/carbon stretching modes, i.e. a change in the conjugation length, this would indicate that a change has occurred in the force constants associated with their vibrations namely $F_{Я}$ and $F_{R^{+}}$. The greatest variation seems to be in $F_{Я}$. The reason can be found in the expressions of $F_{Я}$ and $F_{R^{+}}$, made up from entries in the reduced force constant matrix for the a_g coordinates[5]:

$$F_{Я} = \tfrac{1}{2}(k_R + k_r) - \sum_n \left(- f_R^n - f_r^n + 2 f_{Rr}^n\right) \tag{2.20}$$

$$F_{R^{+}} = \tfrac{1}{2}(k_R + k_r) + \sum_n \left(+ f_R^n + f_r^n + 2 f_{Rr}^n\right) \tag{2.21}$$

Application of 'the rule of alternance' will show that the sum in $F_{Я}$ is always positive, and the sum in $F_{R^{+}}$ remains relatively constant. This rule states that the matrix entries for all f_R and f_r are always negative, and for all f_{Rr} they are positive[5]. The crux of the whole matter is that spectroscopically the $Я$ coordinate, representing the antisymmetric carbon/carbon stretching mode, is the best descriptor of the state of conjugation, as the dependency of the wavelength is well described by $F_{Я}$. Thus, after the spectrum has been obtained, the wavenumber can be related to the force constant $F_{Я}$ from a masterplot of $\nu/F_{Я}$. This masterplot can be obtained by the diagonalisation of the reduced force constant matrix defined by $\mathbf{F}^{a_g}(0)$ [5]. The application of ECC theory has been successfully applied to naturally occurring carotenoid systems[11], showing the generality of the theory. For an in-depth review of ECC theory see the chapter of Gussoni *et al*. in Ref [5].

2.3 References

1. K. Nakamoto, *Infrared and Raman Spectra of Inorganic and Coordination Compounds Part A*, 5th Edition, John Wiley & Sons, New York, 1997.
2. T.G. Spiro (Ed.), *Biological Applications Of Raman Spectroscopy Volume 2*, John Wiley & Sons, New York, 1987.
3. G. Keresztury, *Raman Spectroscopy: Theory* in *Handbook of Vibrational Spetroscopy Volume 1*, J.M. Chalmers, P.R. Griffiths (Eds), John Wiley & Sons, Chichester, 2002.
4. K.I. Mullen, D. Wang, L.G. Krane, K.T. Carron, *Spectroscopy*, 1992, **7**, 24 – 32.
5. M. Gussoni, C. Castiglioni, G. Zerbi, *Spectroscopy of Polyconjugated Materials: Polyacetylene and Polyenes* in *Spectroscopy of Advanced Materials Volume 19*, R.J.H Clark, R.E. Hester (Eds), John Wiley & Sons, Chichester, 1991.
6. G. Zerbi, C. Castiglioni, M. Gussoni, *Synthetic Metals*, 1991, **43**, 3407 – 3412.
7. M. Gussoni, C. Castiglioni, G. Zerbi, *Synthetic Metals*, 1989, **28**, D375 – D380.
8. R.P. Ortiz, M.C.R. Delgado, J. Casado, V. Hernández, O. Kim, H.Y. Woo, J.T.L. Navarrete, *J. Am. Chem. Soc.*, 2004, **126**, 13363 – 13376.
9. V. Hernández, C. Gastiglioni, M. Del Zoppo, G. Zerbi, *Physical Review*, 1994, **50B**, 9815 – 9823.
10. J. Kürti, H. Kuzmany, *Physcial Review*, 1991, **44B**, 597 – 613.
11. M. Veronelli, G. Zerbi, R. Stradi, *J. Raman Spectrosc.*, 1995, **26**, 683 – 692.

Chapter 3

Article submitted to the

Journal of Raman Spectroscopy

Raman Investigation of Pigmentary Molecules in the Molluscan Biogenic Matrix

The pigments of some molluscan shells was identified as carotenoid derivatives. A new relationship was used together with previously reported ones to evaluate the length of conjugation present in the molluscan pigments.

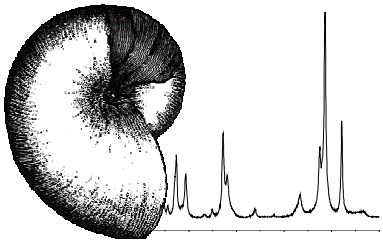

W. Barnard, D. de Waal*

Raman investigation of pigmentary molecules in the molluscan biogenic matrix

Raman investigation of pigmentary molecules in the molluscan biogenic matrix

W. Barnard and D. de Waal*

Department of Chemistry, University of Pretoria, Pretoria 0002, South Africa

3.1 Abstract

Raman spectra of the pigments of several marine mollusc shells have been obtained using the 514.5 nm laser line of an Ar^+ laser. Shell species were chosen to obtain a variety of colour. The spectra obtained for the molluscan pigments indicated that they are polyacetylenic in nature, and from the spectral features it was deduced that the pigments were carotenoids, with unmethylated polyacetylenic backbones of various conjugation lengths. A logarithmic relationship was established between the number of conjugated double bonds (N) and the C=C vibration (ν_1) of previous reported data for finite polyacetylenic systems, and this relationship was used to evaluate the data obtained in this study. The aragonite and calcite phases of $CaCO_3$ were also identified to be present in different species of molluscs.

Keywords: A. Mollusc, B. Raman spectroscopy, C. Polyene, D. Carotenoid, E. Marine Pigment

3.2 Introduction

Carotenoids are the dominant source of colour in nature[1,2] and have been identified in many different body parts of marine invertebrates[1,3,4]. The

* Correspondence to: D. de Waal, Department of Chemistry, University of Pretoria, Pretoria 0002, South Africa. E-mail: danita.dewaal@up.ac.za, fax: +27 12 362 5297.
Contract/grant sponsor: University of Pretoria
Contract/grant sponsor: National Research Foundation.

phylum Mollusca make up the second largest phyla in the animal kingdom, and the shells of the species found under this phylum vary greatly in size, ornamentation and colour. Different colouration scenarios can also occur: One could have a single specie showing a great variation in colour (eg. *Chlamys australis*), or a single shell containing distinct, separate coloured areas (eg. *Conus virgo* & *Drupa morum*). Molluscs are not able to synthesise carotenoids themselves, as these are synthesised afresh only in the plant kingdom[1]. The exact chemical nature of the marine carotenoids of molluscan origin is not known, but they are believed to be carotenoid derivates[5,6,7]. Extraction and limited characterisation has been done on other marine invertebrates such as sponges[8] and the 'By the wind sailor' (*Velella velella*)[9,10]. Carotenoids can chemically be described as conjugated polyacetylenic molecules of finite length, having varied substitution on the terminal ends of the polyene chain, as well as the characteristic four methyl groups substituted on the polyenic backbone.

Raman spectral features have been used extensively for probing the structural nature of carotenoids[5-7,11-13] and of the carotenoids' industrial counterparts, the polyacetylene derivatives[14-19]. Also, the 514.5 nm laser wavelength falls within or close to the energy required for the electronic transition of most carotenoids or polyacetylenic systems, resulting in the Resonance Raman effect that occurs for carotenoids. This feature makes Raman spectroscopy an ideal tool for *in situ* investigation of these pigments in the molluscan matrix.

3.3 Experimental

3.3.1 Molluscan Shells

The molluscan shells in Figure 3-1 were obtained from private collections (*Chlamys australis* – yellow & purple forms, *Conus chaldeus*, *Conus virgo*, *Coralliophila neritiodea*), collected from the South African coastline (*Conus*

tinianus – pink & brown forms), or bought from shell dealers (*Chlamys australis* – orange form, *Drupa morum*, *Pecten raveneli*). Two other molluscan species (*Donax serra*, *Janthina janthina*), shown in Figure 3-2, were chosen for extraction of the organic matrix, by means of decalcification, for further investigation. These two species were freshly collected from the Southern Cape coast of South Africa.

Figure 3-1: Shells of the molluscan species investigated; from the top, left to right: *Chlamys australis* (purple, yellow and orange forms), *Conus tinianus* (pink), *Corallophila neritoidea* (purple), *Drupa morum* (purple), *Conus tinianus* (brown), *Conus chaldeus* (brown), *Pecten raveneli* (maroon), *Conus virgo* (purple).

Figure 3-2: Shells of the two purple coloured molluscan species that were selected for decalcification. *Donax serra* (left) and *Janthina janthina*.

3.3.2 Raman Spectroscopy

The micro-Raman spectra were obtained using a Dilor XY multichannel Raman spectrometer equipped with a liquid nitrogen-cooled CCD detector, and the laser beam focussed on the sample using a confocal Olympus microscope with a 50X objective. All the samples were excited using the 514.5 nm line of a Coherent Innova 300 Ar^+ laser, with a laser output at the source of 100 mW. Approximately 10% of the laser output reached the sample under the microscope. The spectral resolution was 3 cm^{-1}.

3.3.3 Decalcification

A modified procedure from a previously reported method was used[5,6,7]. In this study the shells were not treated with NaOH at any stage of the extraction. The molluscan shells were ground as finely as possible, and stirred overnight in a saturated solution of Na_2EDTA in distilled water. The suspended brown leaflets that were present after decalcification were filtered off and washed with distilled water until no more of the EDTA containing solution was present. The filtrate was then washed with methanol and dried overnight in a desiccator.

The KBr disk was prepared using 100 mg of spectroscopic grade KBr and approximately 2 mg of the organic extract of the *D. serra* specimen. The two components were ground together, and the pellet pressed at 10KPa for 20 minutes.

3.4 Results and Discussion

Figures 3-3, 3-4 and 3-5 show the recorded Raman spectra in the region 600 – 1700 cm^{-1} of the pigmentary molecules of all the molluscan species investigated. All the obtained values for the Raman bands of all species studied are summarised in Table 3-1. Figure 3-6 is the recorded Raman spectrum for the pigment found in *J. janthina* for the region 500 – 4000 cm^{-1},

clearly showing the many combination and overtone bands observed at higher wavenumbers. Similar combination and overtone bands were observed for the other samples studied, and are also included in Table 3-1. Figure 3-7 shows the spectrum obtained for the region 600 – 1700 cm^{-1} of the extracted organic part of the two species *J. janthina* and *D. serra*. These values are also summarised in Table 3-1.

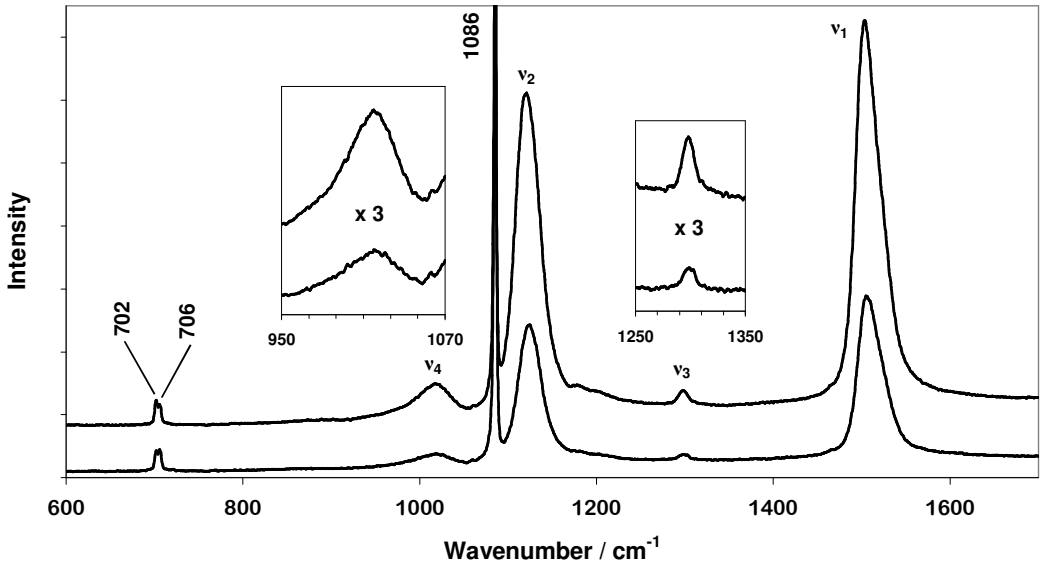

Figure 3-3: Raman spectra of the carotenoid pigments as recorded on the shell for *J. janthina* (top) and *D. serra* (bottom), showing the four fundamental vibrational modes ν_1 – ν_4 of the pigments as described in the text. The $CaCO_3$ phase for the two species is aragonite (bands at 702 and 706 cm^{-1}). The Raman band at 1086 cm^{-1} is the symmetric carbonate stretching mode. The two enlargements are of the two low intensity fundamental bands ν_3 (1298 cm^{-1}) and ν_4 (~1017 cm^{-1}).

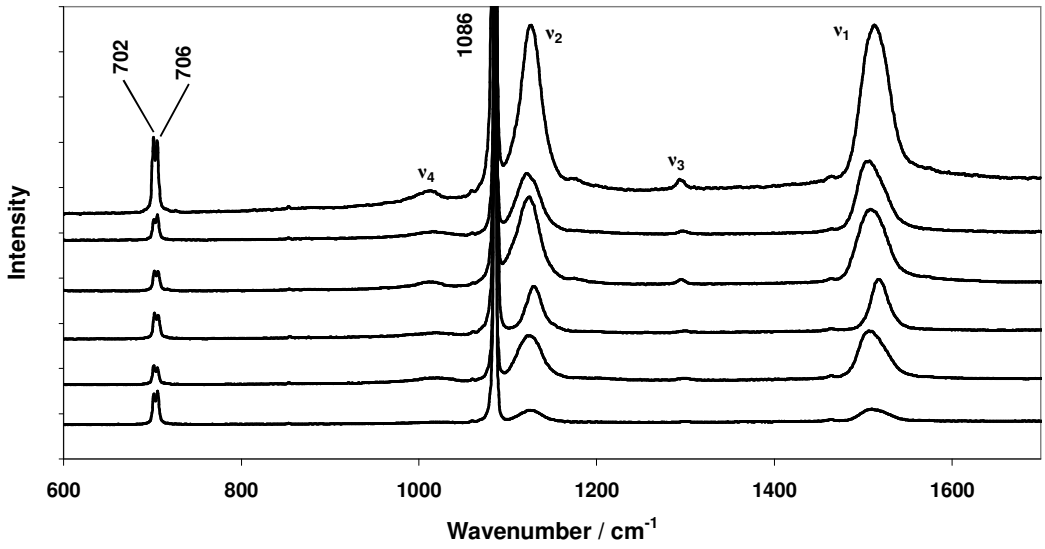

Figure 3-4: Raman spectra of the shell species that were found to consist of the aragonite phase of $CaCO_3$ (bands at 702 and 706 cm^{-1}). From top to bottom the species are: *C. chaldeus* (brown), *C. virgo* (purple siphonal canal), *C. tinianus* (brown), *C. tinianus* (pink), *C. neritoidea* (purple), *D. morum* (purple mouth). The band at 1086 cm^{-1} is typical for the carbonate ion, while the four bands (ν_1, ν_2, ν_3, ν_4) can be attributed to the carotenoidal pigment in the molluscan shells as assigned in Table 3-1.

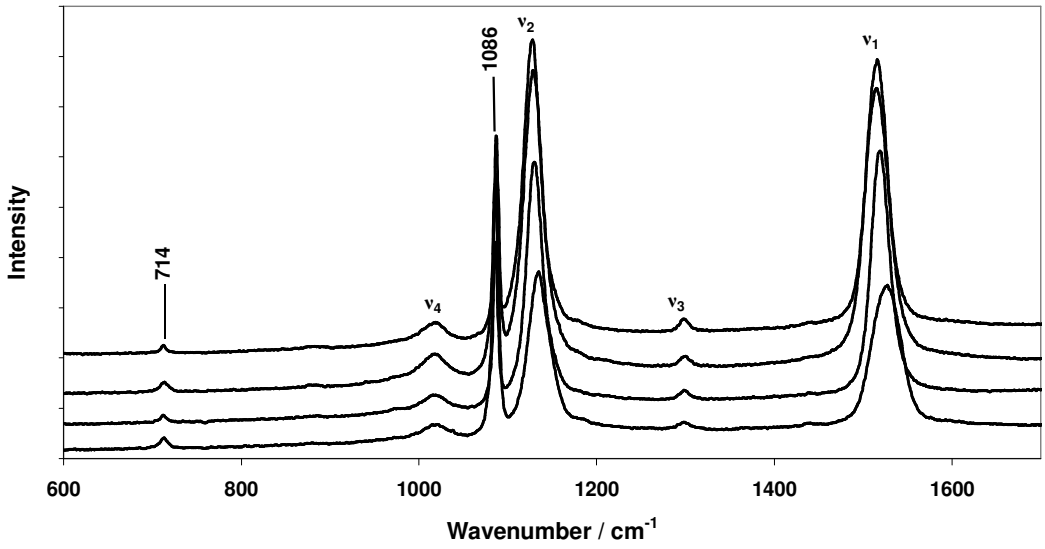

Figure 3-5: Raman spectra of the shell species that were found to consist of the calcite phase of $CaCO_3$ (band at 714 cm^{-1}). From top to bottom the species are: *P. raveneli* (maroon), *C. australis* (purple, orange & yellow). The characteristic carbonate band at 1086 cm^{-1} is observed again, as well as the four fundamental vibrations of the molluscan shell pigment listed in Table 3-1.

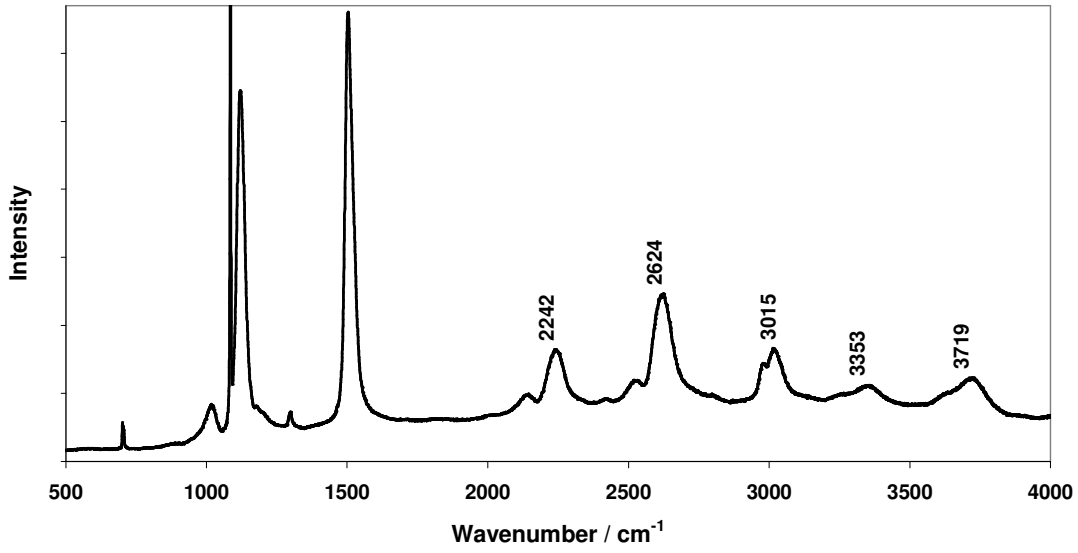

Figure 3-6: The Raman spectrum of the pigment in the carbonate shell matrix of *J. janthina* for the region 500 – 4000 cm^{-1}, showing many combination and overtone bands. The highest intensity bands are indicated in the spectrum, but all bands are reported and assigned in Table 3-1. Similar overtone and combination bands were observed for all the pigments in the molluscan shells and are listed in Table 3-1.

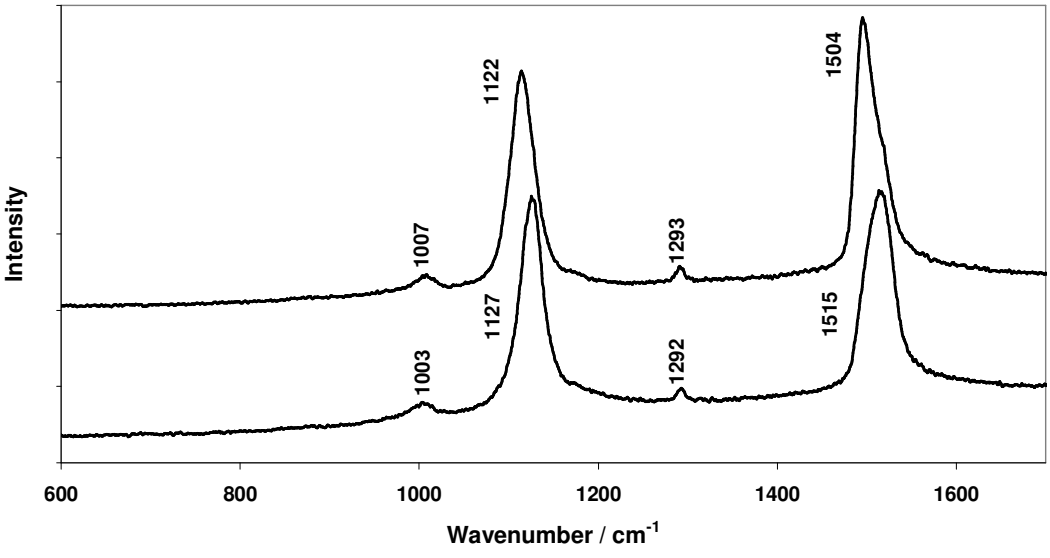

Figure 3-7: The spectrum of the extracted organic part of the shell matrix of *J. janthina* (top) and *D. serra* (bottom). A shift of the bands occur relative to the spectra of the pigments (Figure 3-3) obtained in the carbonate shell matrix (See Table 3-1).

Mollusc / Carotenoid	ν_4	ν_2	ν_3	ν_1	$\nu_2 + \nu_4$	$2\nu_2$	$\nu_2 + \nu_3$	$\nu_1 + \nu_4$	$\nu_1 + \nu_2$	$\nu_1 + \nu_3$	$2\nu_1$	$2\nu_2 + \nu_4$	$\nu_3 + 2\nu_4$	$\nu_1 + \nu_2 + \nu_4$	$\nu_2 + 2\nu_3$
Chlamys australis – yellow	1020	1135	1299	1526	2155	2257	2421	2537	2639	2751	3038	3272	3367	3639	3732
Chlamys australis – orange	1017	1130	1299	1519	2150	2250	2424	2533	2632	-	3032	3266	3364	3650	3739
Chlamys australis – purple	1017	1128	1299	1515	2149	2253	2425	2534	2635	-	3029	3270	3361	3650	3728
Conus chaldeus – brown	1015	1128	1297	1516	2145	2254	2424	2528	2635	-	3028	3253	3356	3626	3733
Conus virgo – purple	1017	1121	1296	1506	2141	2242	2420	2519	2625	2805	3021	3261	3361	3632	3719
Coralliophila neritoidea – purple	1021	1124	1299	1508	2146	2246	2426	2525	2629	2793	3019	3267	3361	3639	3725
Conus tinianus – brown	1011	1124	1295	1509	2143	2250	2422	2521	2627	2801	3025	3270	3356	3643	3720
Conus tinianus – pink	1019	1129	1300	1517	2145	2249	2425	2535	2634	2809	3028	3264	3363	3634	3725
Drupa morum – purple	1019	1125	1298	1510	2140	2248	2414	2531	2629	2756	3028	3250	3364	3624	3732
Pecten raveneli – maroon	1019	1127	1298	1516	2141	2251	2423	2528	2632	2812	3029	3262	3356	3644	3723
Donax serra – purple	1016	1124	1298	1506	2148	2240	2418	2526	2622	2803	3021	3282	3352	3642	3728
Janthina janthina – purple	1018	1120	1298	1501	2145	2242	2421	2527	2619	2796	3015	3264	3353	3633	3719
Donax serra – extract	1003	1127	1292	1515	2138	2248	2410	2516	2632	2810	3024	-	3362	3633	3733
Janthina janthina – extract	1007	1122	1293	1504	2125	2243	2416	2508	2615	-	3007	3244	3340	3626	3703
Tetradesmethyl- β-carotene[a]	-	1133	-	1523	-	2261	-	-	2656	-	3046	-	-	-	-
β-carotene[b,c]	1008	1156	1273	1516	2164	2315	-	2528	2681	-	3048	3319	-	3678	-
Canthaxanthin[b]	1009	1157	1278	1515	2163	2314	-	2527	2673	-	3038	3315	-	3674	-
Astaxanthin[b]	1006	1155	1273	1511	-	-	-	-	-	-	-	-	-	-	-
Zeaxanthin[b]	1009	1157	-	1524	-	-	-	-	-	-	-	-	-	-	-
Lutein[b]	1007	1157	-	1524	-	-	-	-	-	-	-	-	-	-	-
Equinone[b]	1009	1156	1275	1512	-	-	-	-	-	-	-	-	-	-	-
ε,ε-caroten-3,3'-dione[b]	1010	1158	1273	1525	-	-	-	-	-	-	-	-	-	-	-
Spirilloxanthin[c]	1001	1150	-	1508	2150	2297	-	2506	2650	-	3012	3297	-	3646	-

Values and assignments obtained from:
[a] Ref. [20]; [b] Ref. [21]; [c] Ref. [22]

Table 3-1: Raman wavenumbers (cm^{-1}) of the fundamental, combination and overtone bands of the pigmentary molecules in the various molluscan species compared to that of selected synthetic carotenoids.

3.4.1 The Molluscan Shell

The inorganic component of molluscan shells primarily consists of $CaCO_3$[23]. $CaCO_3$ can exist as three polymorphs: calcite, aragonite and vaterite. It is possible to distinguish between the three phases by Raman spectroscopy, as each of them has unique, non-overlapping peaks. Vaterite has bands at 738 cm^{-1} and 750 cm^{-1}, aragonite a doublet at 700 cm^{-1} and 705 cm^{-1}, and calcite a band at 711 cm^{-1} [24]. The most intense band for all three phases occurs at ~1086 cm^{-1}, and is assigned to the symmetric CO_3^{2-} stretching mode[24,25]. Only aragonite and calcite were observed in the molluscan species studied. The Raman spectra of the aragonite shells (*J. janthina*, *D. serra*, *C. chaldeus*, *C. virgo*, *C. tinianus*, *C. neritoidea* and *D. morum*) are shown in Figures 3-3 and 3-4, while Figure 3-5 contains the Raman spectra of the calcite species (*P. raveneli*, *C. australis*).

3.4.2 Polyacetylene

Four main bands are observed in the Raman spectrum of unsubstituted, all *trans*–polyacetylenic molecules[26,27,28]. The two bands of highest intensity are the C=C (ν_1) and C-C (ν_2) stretching modes, which occur between 1450 – 1680 cm^{-1} and 1070 – 1210 cm^{-1} [21,26,29], respectively. These two bands owe their high intensities to resonance enhancement with the 514.5 nm laser line. The ν_3 band is usually observed between 1285 – 1315 cm^{-1} [26,29], and is assigned to the CH=CH in-plane rocking mode of the olefinic hydrogens. The ν_4 band can be found between 1000 – 1015 cm^{-1} [21,27], and is assigned to the CH out-of-plane wagging mode[14,16,27]. The assignment of the ν_4 band was substantiated by Raman studies done on *trans*-acetylene/acetylene-d_2 copolymers, and recently verified by a DFT study of finite, CH_2 terminated polyacetylenes by Fujimori and co-workers, which showed that the Raman inactive in-phase mode of the out-of-plane wagging mode becomes Raman active due to a distortion of the polyenic backbone[27].

3.4.3 Carotenoids

Classical Carotenoids have methyl groups substituted on the polyacetylenic backbone. The Raman spectra of carotenoids contain the four vibrational bands previously mentioned, as well as many other small bands specific to the carotenoid. The regions in which the ν_1, ν_2 and ν_3 bands for carotenoids have been reported are 1480 – 1580 cm^{-1}, 1100 – 1200 cm^{-1} and 1260 – 1290 cm^{-1} respectively[11-13,21,25]. The ν_4 band has been reported to be present between 990 – 1015 cm^{-1} [13,21,25], but is assigned to the rocking mode of the backbone CH_3 groups[13,21]. The spectrum of β-carotene shows two medium-to-low intensity bands at 1008 cm^{-1} and 1018 cm^{-1}. These have been assigned to the out-of-phase and in-phase combinations of the backbone CH_3 rocking modes, respectively, by means of a normal-coordinate analysis of β-carotene[30]. A comparison of this assignment with the spectrum of the unmethylated analogue of β-carotene, tetradesmethyl-β-carotene, found that the absence of the band at 1008 cm^{-1} conclusively supports the assignment[20]. No mention was made of the band at 1018 cm^{-1}, and on inspection of the reported spectrum of tetradesmethyl-β-carotene[20], a weak band is observed at ~1000 cm^{-1}.

3.4.4 The Molluscan Pigments

The two vibrational bands of highest intensity that were recorded between 1501 – 1526 cm^{-1} and 1120 – 1135 cm^{-1} are assigned to the C=C stretching mode (ν_1) and C-C stretching mode (ν_2), respectively[6,7,21]. The band between 1295 – 1300 cm^{-1} is assigned to the CH=CH in-plane rocking mode (ν_3), whereas the ν_4 band between 1015 – 1021 cm^{-1} is assigned to the deformation-activated CH=CH wagging mode[14,27] rather than the methyl rocking mode[6,7]. This assignment is based on the average value of 1017 cm^{-1} observed for the molluscan carotenoids, and corresponds well with the DFT calculated value for CH_2 terminated linear polyacetylenes of 1018 cm^{-1} [27] and the structural deductions which follow.

3.4.5 Analysis of the Four Fundamental Modes

Several structure-related factors can influence the band position of the four fundamentals of the carotenoid pigments in various degrees. The highest intensity bands are mainly associated with the polyene backbone, and the factors determining these band positions are thus also dependent on the nature of the backbone. The most important factors that influence the fundamental mode band positions, mentioned in the literature are: the chemical factors of substitution and the chemical matrix/environment in which the carotenoid is found; conformation, isomerism and electronic factors such as length of conjugation of the polyenic backbone, which affect the extent of the π-delocalisation.

3.4.6 Chemical Factors

3.4.6.1 Substitution

Carotenoids have two main types of substitution, namely terminal and polyene backbone substitution. The type of substitution on the terminal ends of a finite polyene chain seems to have little or no effect on the position of the four fundamental vibrations on comparison of carotenoids that have the same polyene backbone length[13,21], and seems to become even less significant as the polyenic chain increases in length[15]. Terminal substitution and chain conformation are said to give rise to low intensity bands in the 1200 – 1400 cm^{-1} region, but these could be overshadowed by the resonance enhancement of the ν_1 and ν_2 bands[13]. Both the ν_1 and ν_2 bands are sensitive towards substitution of the polyenic backbone. As the π-conjugation decreases due to the deformation of the backbone as a result of substitution, the C=C ν_1 band shifts to a higher wavenumber, and therefore the unsubstituted analogues will have ν_1 at lower wavenumbers[21]. At the same time, if methyl groups are absent from the polyenic backbone, the C-C stretching mode ν_2 wavenumber will be ~20 cm^{-1} lower than that of the

methylated analogue of the same chain length[13]. The ν_1 and ν_2 values for dodecapreno-β-carotene (a methyl substituted, extended polyenic backbone carotenoid) are 1492 cm^{-1} and 1146 cm^{-1} respectively[21]. This example shows that ν_2 is a more reliable indicator for the presence of methyl groups, as ν_2 is not as sensitive towards the extent of the π-conjugation as ν_1. In the present work, the average wavenumber value of the ν_2 band of the molluscan shell carotenoids is 1126 cm^{-1}, which is ~31 cm^{-1} downshifted with respect to the average value of the ν_2 band (~1156 cm^{-1}) of the methylated carotenoids. This shift indicates that an unsubstituted, all-*trans* polyacetylenic molecule is more than likely present in the molluscan shell[6,7,21].

The position of the ν_3 band has also been used as an indicator for polyenic backbone substitution[13]. In the Raman spectrum of conjugated polyenes, the position of the ν_3 band occurs at a lower wavenumber for the unsubstituted chain than for the methyl-substituted chain of the same length[13]. There seems to be no specific wavenumber value that can help to distinguish between methyl substituted or unsubstituted chains of variable lengths. For short-chain polyacetylenes (N = ~4) it seems that ~1300 cm^{-1} could be used as a reference value[29,31,32]. The ν_3 band of carotenoids is found at approximately 1273 cm^{-1} [21]. Corresponding unmethylated analogues should then, according to reference [13], have their ν_3 bands at even lower wavenumbers. Specifically, β-carotene's ν_3 band is at 1273 cm^{-1} [21]. On closer inspection of the spectrum of tetradesmethyl-β-carotene, a possible low intensity ν_3 band is observed at 1280 – 1300 cm^{-1}. This observation contradicts the above statement. Interestingly, it must be said that the possible ν_3 band at 1280 – 1300 cm^{-1} for tetradesmethyl-β-carotene compares well with the ν_3 wavenumber values of 1294 cm^{-1} for infinite (C=C > 100) unsubstituted polyacetylene[16], or ~1292 cm^{-1} for finite polyacetylene systems[15]. Thus, the above statement from reference [13] seems to hold only for short polyene systems and not for those that have carotenoidal nature and lengths (C=C > ~8). The average value of ν_3 for the molluscan carotenoids in this work is 1298 cm^{-1}, which compares well with that reported for the

aforementioned infinite and finite unsubstituted polyacetylene systems, substantiating the earlier deduction that the molluscan carotenoid backbones are unsubstituted.

3.4.6.2 The Chemical Matrix

Carotenoids are not usually found in the free form in nature but rather as complexed with some form of protein[4,9-12]. These complexes, or carotenoproteins, commonly differ greatly in colour relative to that of the uncomplexed carotenoid. A prime example is the carotenoprotein α-crustacyanin that contains the carotenoid astaxanthin. It has a bathochromic shift in its absorption spectrum of ~150 nm from the free to complexed carotenoid[9,33]. The crystal structure of α-crustacyanin has been reported[9], showing the strained nature of the backbone and the terminal rings of the astaxanthin molecule relative to the uncomplexed structure. This strain is also observed in the Raman spectrum of α-crustacyanin[11]. Upon complexation of the carotenoid with a protein, the most important change in the spectrum is the appearance of many more vibrational bands[11-13,33], and the downshift of the ν_1 band, which is rationalised by the increase in π-delocalisation[11]. None of these extra bands were observed in the obtained spectra of the molluscan carotenoids, thus making the possibility of interaction between the carotenoid and the conchoilin protein of the shell highly unlikely. A $CaCO_3$-carotenoid complex has been proposed to exist in the calcareous skeletons of corals[34,35], and some shells[7]. This would also be a more plausible explanation for the currently reported molluscs.

Upon extraction of the organic component from the shells of *J. janthina* and *D. serra*, the colour changed from purple to golden brown. On comparison of Figure 3-3 with Figure 3-7 slight shifts were observed in the Raman spectra for all four of the fundamental modes. The ν_1 and ν_2 bands shifted to a higher wavenumber, and the ν_3 and ν_4 showed a downward shift. These changes in the band positions could possibly be explained by the orientation of the

carotenoids in the biogenic $CaCO_3$ matrix, as the structure of the aragonite biogenic matrix is mostly crossed lamellar[36] and the partial orientation of a carotenoid has been observed in the feather of the bird species *Cyanoramphus novalandiae*[21]. It is therefore likely that the carotenoid might orientate itself in a lamellar packed fashion as well in the $CaCO_3$ matrix. Also, the position of the ν_1 band for carotenoids has been observed to differ in solution from the solid form[21]. The result when the organic extract of *D. serra* used in this study was compressed in a KBr disk was that the ν_1 band position shifted 4 cm^{-1} towards a lower wavenumber value (towards the ν_1 band position obtained for the pigment on the shell) relative to the position of the ν_1 band of the extract – a positive indication for preferential orientation of the carotenoid in the biogenic $CaCO_3$ matrix.

3.4.7 Electronic Factors

The extent of the π-delocalisation, i.e. the effective length of conjugation, mainly depends on a few factors. The v_1 wavenumber is affected most by the extent of the π-delocalisation[6,7,21,26], whereas no appreciable change is observed for the v_3 and v_4 vibrational bands[11,21,30].

3.4.7.1 Conjugation Length

Schaffer et al. showed that on going from a 3-ene to 12-ene tert-butyl capped all-trans conjugated system, the v_1 band downshifted by ~133 cm^{-1} while the v_2 and v_3 bands only varied by approximately 15 cm^{-1} and 3 cm^{-1} each[15]. Similar observations have been made on shorter polyene chains[29,31,37], and confirmed with DFT calculations on all-trans polyene chains of the kind $H(CH{=}CH)_nH$ with n = 1 – 12[38].

3.4.7.2 Isomerism

The bulk of carotenoids have an all-trans configuration of the polyenic backbone, but some cis-carotenoids have been reported[39]. A normal-coordinate analysis has also been done on 15-cis-β-carotene[30], and on comparison with the all-trans isomer, the ν_1 band position for the cis isomer is at a higher value. This indicates the loss of some π-delocalisation of the polyenic backbone i.e. the length of the trans-conjugation segment in the molecule will be shorter, resulting in the ν_1 band position to shift to a higher wavenumber[13,30].

3.4.7.3 Conformation

If the conformation of the polyenic backbone was to deviate from planarity some of the π-delocalisation is lost, resulting in the ν_1 band to shift to a higher wavenumber. On comparison of the ν_1 band position of some carotenoids in the solid state and in solution[21], one sees that the solid-state value is lower than that in solution, and is again indicative of some loss of the π-delocalisation in solution[21]. For β-carotene this shift is ~9 cm^{-1} [30].

Taking all three these factors into account (conjugation length, isomerism and chain conformation), it then appears that the band position of ν_1 is a good indicator of the 'effective conjugation length', rather than a rigid predictor of the number of conjugated double bonds[21,25,26].

3.4.8 Conjugation Length of the Molluscan Carotenoids

Because of the dependence of the ν_1 on the 'effective conjugation length' (maximum number of conjugated double bonds) and the ground electronic state[7,40], empirical correlations for the possible number of conjugated double bonds (N), the C=C vibrational mode (ν_1), the C-C vibrational mode (ν_2) and the absorption wavelength in solution have been obtained[6,7,14,40]. These

correlations have been used to make predictions about carotenoids of which the spectra were obtained *in situ*[25] or extracted[6,7]. The first of these relationships was published for polyacetylene, and relates the value of the ν_1 band with the number of conjugated double bonds, N [14].

$$\nu_1 = 1459 + \frac{720}{N+1} \qquad (\text{cm}^{-1}) \qquad (3.1)$$

Evaluation of reported experimental Raman data of carotenoids with CH_3 groups present on their polyene backbones using Equation 3.1, shows that N will be overestimated[6,7]. Similar mathematical relationships, for which the equations are given here, were obtained for the series of *tert*-butyl capped polyacetylenes for both the ν_1 and ν_2 bands[15]:

$$\nu_1 = 1438 + \frac{830}{N} \qquad (\text{cm}^{-1}) \qquad (3.2)$$

and

$$\nu_2 = 1082 + \frac{476}{N} \qquad (\text{cm}^{-1}) \qquad (3.3)$$

Equations 3.2 and 3.3 were obtained using only the data reported for *tert*-butyl capped polyacetylenes having $7 \leq N \leq 12$ and $8 \leq N \leq 12$ respectively[15]. As previously stated, the value of the ν_1 vibration would be an indication of the 'effective conjugation length' rather than of a fixed number of double bonds. This concept of 'effective conjugation length' is best described by the ECC (effective conjugation coordinate) theory as reviewed by Zerbi *et al*[15]. ECC theory states that the $Я$ mode (which is a combination of a_g symmetry coordinates) is the most enhanced of the totally symmetric modes, and the wavenumber of the a_g modes is dependent on the force constant $F_Я$[25,26]. $Я$ (the effective conjugation coordinate) is pivotal in expressing the state of conjugation[26,41]. Thus, a much better description of the conjugation state can

be obtained by comparing the force constant $F_{\mathcal{A}}$ and the wavenumber of the a_g modes (eg. ν_1 or ν_2)[21,26]. To obtain such a master curve for comparison, a diagonalisation of the force constant matrix for the a_g coordinates, $\mathbf{F}^{a_g}(0)$, needs to be done[26].

The values obtained from Equations 3.1 – 3.3 for N for the molluscan carotenoids in this study are listed in Table 3-2. The plot of ln(1/N) vs ν_1 for the data reported in reference [15], resulted in a linear relation with a least square regression analysis (R^2) value of 0.9987 for $3 \leq N \leq 12$. Figure 3-8 shows the graph and the linear relationship,

$$\nu_1 = 97.07 \ln(1/N) + 1745 \quad (\text{cm}^{-1}) \qquad (3.4).$$

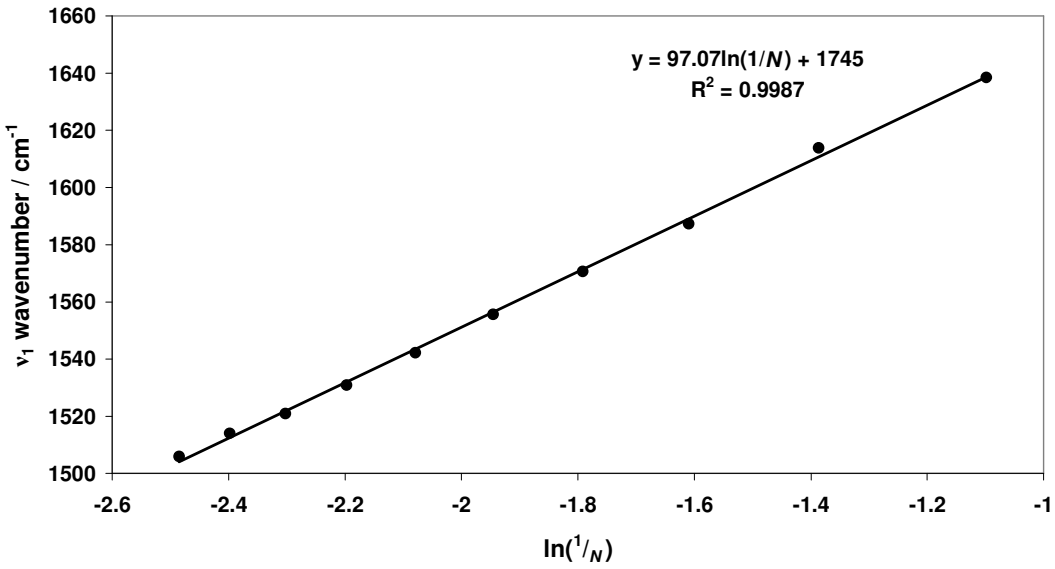

Figure 3-8: A plot of ln(1/N) vs the ν_1 wavenumber, where N is the number of conjugated double bonds, for the series of *tert*-butyl capped polyacetylenes with $3 \leq N \leq 12$ obtained from the data of Reference [15]. This correlation should be more accurate, as it contains more data points as previously reported correlations obtained from the same set of data[15]. This relationship is used in the text as Equation 3-4.

Mollusc	ν_1	ν_2	Eq. 3.1	Eq. 3.2	Eq. 3.3	Eq. 3.4	Fig. 3-9
Chlamys australis – yellow	1526	1135	10	9	9	10	9
Chlamys australis – orange	1519	1130	11	10	10	10	10
Chlamys australis – purple	1515	1128	12	11	10	11	10-11
Conus chaldeus – brown	1516	1128	12	11	10	11	10-11
Conus virgo – purple	1506	1121	14	12	12	12	12
Coralliophila neritoidea – purple	1508	1124	14	12	11	12	11-12
Conus tinianus – brown	1509	1124	13	12	11	11	11-12
Conus tinianus – pink	1517	1129	11	11	10	11	10
Drupa morum – purple	1510	1125	13	12	11	11	11
Pecten raveneli – maroon	1516	1127	12	11	11	11	11
Donax serra – purple	1506	1124	14	12	11	12	11-12
Janthina janthina – purple	1501	1120	16	13	13	12	12-13
Donax serra – extract	1515	1127	12	11	11	11	11
Janthina janthina – extract	1504	1122	15	13	12	12	12

Table 3-2: Comparison of the different mathematical relations previously reported (Eq's. 3.1 – 3.3) with the presently reported Eq. 3.4 compared to the possible prediction of the number of double bonds (N) obtained from Fig. 3-9 for the pigments in the molluscan samples.

This relationship should be better than Equations 3.2 and 3.3 as it derives from a larger data set. The number of double bonds predicted by Equation 3.4 is listed in comparison with Equations 3.1 – 3.3 in Table 3-2. Figure 3-9 shows a plot similar to the one published by Veronelli *et al.* to compare the *tert*-butyl conjugated systems to the studied molluscan carotenoids. Comparing the values predicted by Equations 3.1 – 3.4 with the values estimated for the molluscan carotenoids in Figure 3-9, shows that Equation 3.1 overestimates the number of double bonds. Comparison of the values obtained for N from Equations 3.2, 3.3 and 3.4 with the molluscan values in Figure 3-9, it would seem that Equation 3.4 gives a more accurate simulation of the obtained data. Possible reasons could be that even though Equation 3.2 is based on the position of the ν_1 (C=C) band, it was fitted only for a region that seems linear, which could account for the few incorrect values, whereas Equation 3.3 is based on the position of the ν_2 (C-C) band position, which is not as sensitive towards substitution as the C=C stretching vibration (a total shift of ~15 cm^{-1} going from the 3-ene to the 12-ene[15]), thus accounting for the less accurate prediction.

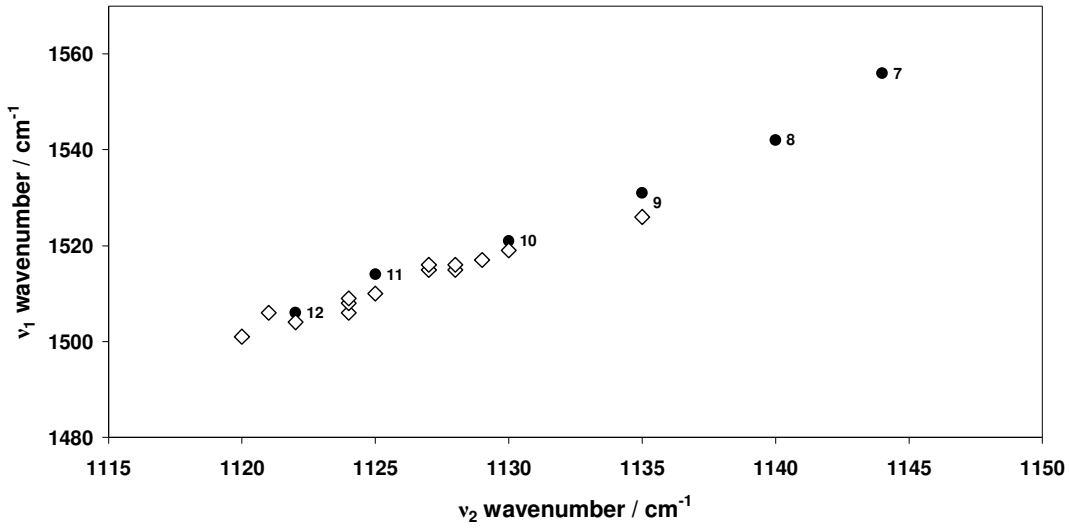

Figure 3-9: Plot of the C=C wavenumber (ν_1) versus C-C wavenumber (ν_2) similar to that obtained by Veronelli *et al.*, for bird feathers, showing the relation of the data obtained for the molluscan carotenoids (◇) to that of known conjugation length *tert*-butyl capped polyacetylenes[15] (●). The number next to each ● indicates the number of conjugated double bonds present in that specific *tert*-butyl capped polyacetylene.

3.5 Conclusions

The Raman spectra indicated that all the bivalves except for *D. serra* were found to be calcite, and all the gastropods were aragonite. From the spectral features it was found that the molluscan pigments in the present study were unsubstituted polyacetylenes, possibly of the carotenoid class of compounds, and are probably not associated with the conchoilin protein in the shell. The pigments are probably found in a preferred orientation in the shell matrix, and upon evaluation of a new correlation, Equation 3.4, between the C=C wavenumber (ν_1) and the number of conjugated double bonds, it was found that the pigments probably contain between 10 – 12 conjugated double bonds. No plausible explanation can be given for the great diversity in colour, even though the number of double bonds only differed by a maximum of two. As a result of the structural deductions, the assignment of the band at ~1015

cm^{-1} to being an activated CH=CH wagging mode rather than a CH_3 rocking mode as previously reported[6,7], is accepted.

An interesting observation that was made is the difference in the reported spectrum of *V. velella*[10] and that obtained for *J. janthina*. *J. janthina* lives in the neuston (top 10 – 20 cm of the ocean's surface), drifting intercontinentally on the ocean's currents. Many other invertebrates of the genusses *Physalia*, *Glauca*, *Porpita*, and specifically the species *V. velella*, live in symbiosis with the purple mollusc in the neuston. Most are either transparent or coloured blue or purple. *J. janthina* is a carnivorous mollusc feeding on these species, and it can therefore be postulated that it sources its own colour from these invertebrates. On comparison of the Raman spectrum of the pigment in *V. velella* with that obtained for *J. janthina* it was seen that they differ in band positions, and there are extra bands observed in the spectrum of *V. velella*. The spectrum of *V. velella* was reported as being that of an astaxanthin-protein complex[10]. This could therefore be a possible indication that the mollusc is chemically alterering the carotenoid, for reasons unknown.

3.6 Acknowledgements

The financial support by the University of Pretoria and the National Research Foundation, Pretoria, is gratefully acknowledged. The Conchological Society of South Africa for help in specimen identification is acknowledged, as well as Prof. JCA Boeyens for helpful discussions of the work.

3.7 References

1. Wilbur KM, Yonge CM (eds). *Physiology of Mollusca*: Vol. 2. *Pigmentation of Molluscs.* Academic Press: New York, 1966.
2. Hudon J. *Biotech. Adv.* 1994; **12**: 49.

3. Fox DL. *Animal Biochromes and Structural Colours.* Cambridge University Press, 1953.
4. Cheesman DF, Lee WL, Zagalsky PF. *Biol. Rev.* 1967; **42**: 132.
5. Merlin JC, Delé-Dubois ML. *Bull. Soc. Zool. Fr.* 1983; **108**: 289.
6. Merlin JC. *Pure Appl. Chem.* 1985; **57**: 785.
7. Merlin JC, Delé-Dubois ML. *Comp. Biochem. Physiol.* 1986; **84B**: 97.
8. Santoro P, Guerriero V, Parisi G. *Comp. Biochem. Physiol.* 1990; **97B**: 645.
9. Chayen NE, Boggon TJ, Raftery J, Helliwell JR, Zagalsky PF. *Acta Crystallogr.* 1999; **55D**: 266.
10. Clark RJH, D'Urso NR, Zagalsky PF. *J. Am. Chem. Soc.* 1980; **102**: 6693.
11. Weesie RJ, Merlin JC, De Groot HJM, Britton G, Lugtenburg J, Jansen FJHM, Cornard JP. *Biospectroscopy* 1999; **5**: 358.
12. Weesie RJ, Merlin JC, Lugtenburg J, Britton G, Jansen FJHM, Cornard JP. *Biospectroscopy* 1999; **5**: 19.
13. Merlin JC. *J. Raman Spectrosc.* 1987; **18**: 519.
14. Kuzmany H. *Phys. Stat. Sol.* 1980; **97B**: 521.
15. Schaffer HE, Chance RR, Silbey RJ, Knoll K, Schrock RR. *J. Chem. Phys.* 1991; **94**: 4161.
16. Takeuchi H, Furukawa Y, Harada I, Shirakawa H. *J. Chem. Phys.* 1984; **80**: 2925.
17. Schen MA, Chien JCW, Perrin E, Lefrant S, Mulazzi E. *J. Chem. Phys.* 1988; **89**: 7615.
18. Zerbi G, Castiglioni C, Gussoni M. *Synthetic Metals* 1991; **43**: 3407.
19. Gussoni M, Castiglioni C, Zerbi G. *Synthetic Metals* 1989; **28**: D375.
20. Okamoto H, Saito S, Hamaguchi H, Tasumi M, Eugster CH. *J. Raman Spectrosc.* 1984; **15**: 331.
21. Veronelli M, Zerbi G, Stradi R. *J. Raman Spectrosc.* 1995; **26**: 683.
22. Okamoto H, Sekimoto Y, Tasumi M. *Spectrochim. Acta* 1994; **50A**: 1467.
23. Wilbur KM, Yonge CM (eds). *Physiology of Mollusca*: Vol. 1. *Shell Formation and Regeneration.* Academic Press: New York, 1964.

24. Kontoyannis CG, Vagenas NV. *The Analyst* 2000; **125**: 251.
25. Withnall R, Chowdhry BZ, Silver J, Edwards HGM, De Oliveira LFC. *Spectrochim. Acta* 2003; **59A**: 2207.
26. Clark RJH, Hester RE (eds). *Spectroscopy of Advanced Materials*: Vol. 19. *Spectroscopy of Polyconjugated Materials: Polyacetylene and Polyenes.* John Wiley & Sons: Chichester, 1991.
27. Fujimori K, Sakamoto A, Tasumi M. *Macromol. Symp.* 2004; **205**: 33.
28. Fujiwara M, Hamaguchi H, Tasumi M. *Appl. Spectrosc.* 1986; **40**: 137.
29. Abo Aly MM, Baron MH, Favrot J, Romain F, Revault M. *Spectrochim. Acta* 1984; **40A**: 1037.
30. Saito S, Tasumi M. *J. Raman Spectrosc.* 1983; **14**: 310.
31. Abo Aly MM, Baron MH, Coulange MJ, Favrot J. *Spectrochim. Acta* 1986; **42A**: 411.
32. McDiarmid R, Sabljić A. *J. Phys. Chem.* 1987; **91**: 276.
33. Britton G, Weesie RJ, Askin D, Warburton JD, Gallardo-Guerroro L, Jansen FJ, De Groot HJM, Lugtenburg J, Cornard JP, Merlin JC. *Pure Appl. Chem.* 1997; **69**: 2075.
34. Ronneberg H, Borch G, Fox DL, Liaaen-Jensen S. *Comp. Biochem. Physiol.* 1979; **62B**: 309.
35. Berger H, Ronneberg H, Borch G, Liaaen-Jensen S. *Comp. Biochem. Physiol.* 1982; **71B**: 253.
36. Dauphin Y, Denis A. *Comp. Biochem. Physiol.* 2000; **126B**: 367.
37. Lee JY, Lee SJ, Kim KS. *J. Chem. Phys.* 1997; **107**: 4112.
38. Schettino V, Gervasio FL, Cardini G, Salvi PR. *J. Chem. Phys.* 1999; **110**: 3241.
39. Koyama Y, Takii T, Saiki K, Tsukida S. *Photobiochem. Photobiophys.* 1983; **5**: 209.
40. Rimai L, Heyde ME, Gill D. *J. Am. Chem. Soc.* 1973; **95**: 4493.
41. Granville MF, Kohler BE, Snow JB. *J. Chem. Phys.* 1981; **75**: 3765.

Chapter 4

Conclusions

4.1 Structure of the Pigment

From the position of the ν_1-ν_4 vibrational bands in the obtained Raman spectra of the molluscan shells, it was deduced that the pigmentary molecules are of a polyacetylenic nature, most probably of the carotenoid class of compounds. Most important, is that the spectral data indicates that the polyacetylenic chain is unsubstituted, therefore lacking the four methyl groups that are usually associated with the backbone of a carotenoid (See Figure 1-1). This has only been reported in four previously published papers[1-4]. No evidence could be found in the spectra to help in determining the chemical nature of the terminal groups of the polyacetylenes.

Association with the conchoilin protein seems highly unlikely, as there was no spectral evidence to support this. Also, comparison of the Raman spectra of the extracted organic part of *D. serra* and *J. janthina* with that of the pigment *in situ* in the shell, shows that some conformational changes of the backbone could have occurred, even though the colour changed dramatically from purple to golden brown. No dramatic spectral shifts occurred similar to those usually observed for a carotenoid relative to its protein-complexed form[5].

For the extracted organic component it was found that the length of conjugation was shortened, but this is not sufficient enough to explain the dramatic colour change of the organic extract (golden brown) relative to the pigment in the molluscan matrix (purple). Posssible reasons for this colour change could rather be interaction with the matrix or other pigmentary

molecules, but not interaction with the conchoilin protein as the Raman spectra did not indicate any such interaction.

4.2 Length of Conjugation of the Pigments

Using a new correlation (Equation 3-4) obtained from previously reported data, the number of conjugated double bonds in the molluscan pigments were predicted to range from ten to twelve double bonds. This correlation (Equation 3-4) has a R^2 = 0.9987, which makes it more reliable than the previously reported correlations. The ten to twelve double bond range predicted for the pigments investigated here, is a relatively small structural change for such a diversity of colour, and therefore conjugation cannot be the only contributor to the colour of the molluscan pigment. Most probably other factors could include: the nature of the terminal groups, interaction with the shell matrix and concentration of the pigment in the biogenic matrix. A more detailed discussion of the conclusions pertaining to the length of conjugation and the correlation can be found in Chapter 3 under Sections 3.4 and 3.5.

4.3 Conjugation Length and Colour

Empirically comparing the colour of the shell with the prediction of the conjugation length, it is seen that the observations fit well with what one would classically expect. The shells range from purple through yellow, and therefore the shells that are coloured purple are absorbing the longer wavelength colours (yellows, reds and oranges), thus indicating that they should have the longer length of conjugation, similarly this should hold for the yellow and orange coloured shells, and one expects them to have the shorter conjugation length to absorb the shorter light wavelengths. To easier see this correlation it is represented in Figure 4-1. This is a very simplistic view, but always reassuring to see that what one intuitively expects does occur.

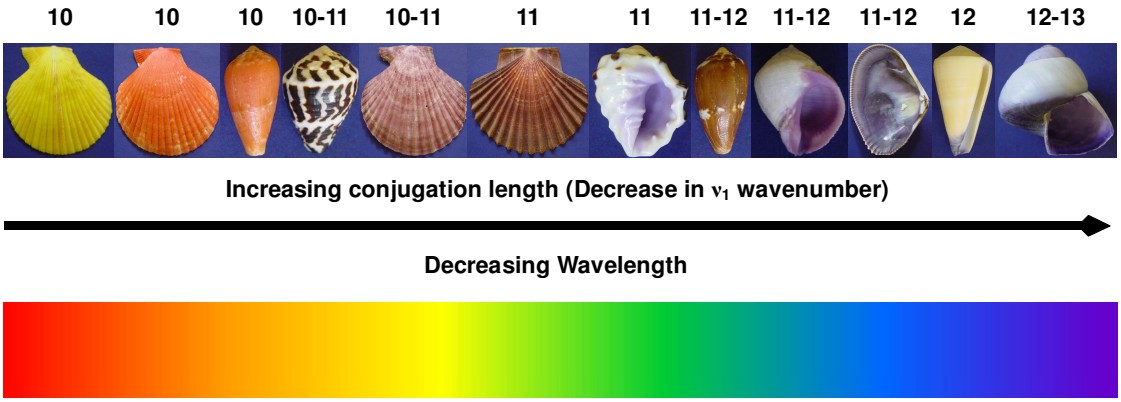

Figure 4-1: Schematic showing the empirical relation of the shell colour relative to the C=C (ν_1) predicted length of conjugation from Figure 3-9. Notice that the yellow shell (*C. australis*) seems not to fit with the trend, but that it's number of double bonds are very similar to the two orange species.

4.4 The $CaCO_3$ of the Biogenic Matrix

Of the three phases of $CaCO_3$ only aragonite and calcite was identified. On classifying the species into their phases it was found that all the gastropods (*J. janthina*, *C. chaldeus*, *C. virgo*, *C. tinianus*, *C. neritoidea* and *D. morum*) were aragonite, and all the bivalves (*P. raveneli*, *C. australis*) were calcite, except for the bivalve *D. serra* which was aragonite. Aragonite is known to be thermodynamically less stable, and more soluble than calcite under pressure. The locales of the aragonite species are mostly cold-water current regions. The calcite species have their main locations in warm, tropical regions, lending itself as a possible factor for the choice of carbonate phase. If one of the contributing factors for the choice of phase is the temperature, it could also explain the exception of the bivalve *D. serra* which is a cold-water bivalve found mainly of the Southern coast of South Africa.

4.5 References

1. M. Veronelli, G. Zerbi, R. Stradi, *J. Raman Spectrosc.*, 1995, **26**, 683.
2. J.C. Merlin, M.L. Delé-Dubois, *Bull. Soc. Zool. Fr.*,1983, **108,** 289 - 301.
3. J.C. Merlin, *Pure Appl. Chem.* 1985, **57**, 785 - 792.
4. J.C. Merlin, M.L. Delé-Dubois, *Comp. Biochem. Physiol.*,1986, **84B**, 97 – 103.
5. R.J. Weesie, J.C. Merlin, J. Lugtenburg, G. Britton, F.J.H.M. Jansen, J.P. Cornard, *Biospectroscopy*, 1999, **5**, 19 – 33.